Universidade do Minho
Escola de Medicina

Helena Maria Vilaça Faria

Mesenchymal Stem Cells Secretome – derived exosomes: Biological Nanovesicles for the treatment of Parkinson's Disease?

Julho de 2019

Helena Maria Vilaça Faria **Mesenchymal Stem Cells Secretome – derived exosomes: Biological Nanovesicles for the treatment of Parkinson's Disease?**

UMinho | 2019

Universidade do Minho
Escola de Medicina

Helena Maria Vilaça Faria

Mesenchymal Stem Cells Secretome – derived exosomes: Biological Nanovesicles for the treatment of Parkinson's Disease?

Dissertação de Mestrado
Mestrado em Ciências da Saúde

Trabalho Efetuado sob a orientação da
Doutor Fábio Gabriel Rodrigues Teixeira
e do
Professor Doutor António José Braga Osório Gomes Salgado

Julho de 2019

ACKNOWLEDGMENTS

Agradeço a todos os que, direta ou indiretamente, estiveram presentes no decorrer desta tese e me apoiaram. O meu mais profundo e sincero obrigado, sem a vossa ajuda não conseguiria.

"One, remember to look up at the stars and not down at your feet. Two, never give up work. Work gives you meaning and purpose and life is empty without it. Three, if you are lucky enough to find love, remember it is there and don't throw it away."

— Stephen Hawking

This work was supported by the Portuguese Foundation for Science and Technology (FCT): IF Development Grant (IF/00111/2013) to AJ Salgado and Post-Doctoral Fellowship to FG Teixeira (SFRH/BPD/118408/2016). This work was funded by FEDER, through the Competitiveness Internationalization Operational Programme (POCI), and by National funds, through the Foundation for Science and Technology (FCT), under the scope of the project POCI-01-0145-FEDER-029751. This article has also been developed under the scope of the project NORTE-01-0145-FEDER-000023, supported by the Northern Portugal Regional Operational Programme (NORTE 2020), under the Portugal 2020 Partnership Agreement, through the European Regional Development Fund (FEDER). This work has been funded by FEDER funds, through the Competitiveness Factors Operational Programme (COMPETE), and by National funds, through FCT, under the scope of the project POCI-01-0145-FEDER-007038.

STATEMENT OF INTEGRITY

I hereby declare having conducted this academic work with integrity. I confirm that I have not used plagiarism or any form of undue use of information or falsification of results along the process leading to its elaboration.

I further declare that I have fully acknowledged the Code of Ethical Conduct of the University of Minho.

RESUMO

A doença de Parkinson (DP) é a segunda doença neurodegenerativa mais comum no mundo. É caracterizada clinicamente por complicações motoras severas causadas pela degeneração progressiva de neurónios dopaminérgicos (DAn) e pelo declínio de dopamina. Os tratamentos atuais focam-se no uso de estratégias farmacológicas como a administração de levodopa, focando-se apenas na atenuação dos sintomas motores e não na regeneração dos DAn. Portanto, o desenvolvimento de estratégias regenerativas é essencial, as quais podem levar a ganhos promissores na investigação translacional da DP. O secretoma de células estaminais mesenquimatosas humanas (hMSCs) tem sido proposto como uma ferramenta terapêutica promissora para a DP, dado a sua capacidade de modular a sobrevivência de DAn. Enquanto que com a fração proteica, o nosso laboratório já identificou proteínas promissoras com ações terapêuticas na DP, levando a melhorias histológicas e comportamentais, o potencial da sua fração vesicular/exossomal ainda permanece pouco explorada. As vesículas derivadas das hMSCs são capazes de atuar como nanopartículas biológicas com efeitos benéficos em diferentes condições patológicas, incluindo na DP. Assim sendo, o objetivo deste trabalho foi isolar e caracterizar os exossomas derivados do secretoma de hMSCs, assim como avaliar o seu impacto na sobrevivência, e na diferenciação neuronal através do uso de modelos *in vitro* e *in vivo* da DP. Os resultados demonstraram que foi possível o isolamento de exossomas por um protocolo de ultracentrifugação diferencial, ao caracterizar as amostras através da técnica Dynamic Light Scattering (DLS). Adicionalmente, ensaios *in vitro*, com o objetivo de avaliar a diferenciação neuronal para marcadores DCX e MAP-2, revelaram que a fração exossomal foi capaz de induzir diferenciação de células progenitoras neurais (NPCs) ao mesmo nível que o secretoma total, enquanto que a fração proteica não foi capaz de induzir tal efeito. Num modelo de DP de 6-OHDA, foi possível observar que as diferentes frações do secretoma induziram um efeito positivo na performance motora e na análise histológica, apesar de apresentarem efeitos distintos, indicando assim que o secretoma e as suas diferentes frações podem influenciar diferentes mecanismos e vias. Em suma, é possível concluir que o secretoma de hMSCs e as suas frações podem ser moduladores de diferentes mecanismos de neuroregeneração, abrindo uma oportunidade para o seu uso como estratégia terapêutica no tratamento da DP.

PALAVRAS CHAVE: Doença de Parkinson; Células Estaminais Mesenquimatosas; Secretoma; Exossomas

ABSTRACT

Parkinson's Disease (PD) is the second most prevalent neurodegenerative disorder in the world. It is clinically characterized by severe motor complications caused by the progressive degeneration of dopaminergic neurons (DAn) and dopamine loss. Current treatment focus on mitigating the symptoms through levodopa administration, rather than preventing DAn damage. Therefore, the development of regenerative strategies is essential, which can lead to promising gains on PD translational research. Human mesenchymal stem cells (hMSCs) secretome has been proposed as a promising therapeutic tool, given their ability to modulate DAn survival. While with the protein fraction, our lab has already identified promising proteins with therapeutic actions on PD, leading to histological and behavioral improvements, the potential of its vesicular/exosomal fraction still remains not fully understood. hMSCs – derived vesicles are able to act as biological nanoparticles with beneficial effects in different pathological conditions, including PD. Therefore, the aim of this work was to isolate hMSCs secretome-derived exosomes and characterize its fraction, as well as assess their impact on neuronal survival, and differentiation through the use of *in vitro* and in *in vivo* models of PD. Our results have demonstrated that we were able to isolate hMSCs-derived exosomes by a differential ultracentrifugation protocol, when characterizing exosomal samples through Dynamic Light Scattering (DLS) method. Concerning *in vitro* assays assessing neuronal differentiation to DCX and MAP-2 markers, results revealed that the exosomal fraction was able to induce neural progenitor cells (NPCs) differentiation at the same levels as the whole secretome, while the protein separated fraction was not able to induce such effect. In a 6-OHDA rat model of PD, we have observed that hBM-MSCs secretome and its derived fractions displayed a positive impact on animals' motor and histological performance, although presenting distinct effects, thereby indicating that the secretome and its different fractions may impact different mechanisms and pathways. Overall, we concluded that the use of the secretome collected from hBM-MSCs and its different fractions might be active modulators of different neuroregeneration mechanisms, opening a door for their future use as therapeutical strategies in the treatment of PD.

KEYWORDS: Parkinson's Disease; Mesenchymal Stem Cells; Secretome; Exosomes

TABLE OF CONTENTS

LIST OF ABBREVIATIONS

ATB: Apomorphine Turning Behavior

ANS: Autonomic Nervous System

BNM: Basal Nucleus of Meynert

BBB: Blood Brain Barrier

COMT: Catechol-o-methyl Transferase

CNS: Central Nervous System

CYL: Cylinder

Cys-C: Cystatin-C

DAB: 3,3'-diaminobenzidine tetrahydrochloride

DBS: Deep Brain Stimulation

DAn: Dopaminergic Neurons

DMV: Dorsal Motor Nucleus of the Vagus

DCX: Doublecortin

DLS: Dynamic Light Scattering

EBs: Embryoid Bodies

EFs: Embryoid Fibroblasts

EPM: Elevated Plus Maze

ESC: Embryonic Stem Cells

ENS: Enteric Nervous System

EVs: Extracellular Vesicles

FCS: Fetal Calf Serum

FGF20: Fibroblast Growth Factor 20

FST: Forced Swim Test

hBM-MSCs: Human Bone Marrow-Derived Mesenchymal Stem Cells

hNPCs: Human Neural Progenitor Cells

H_2O_2: Hydrogen Peroxidase

6-OHDA: 6-hydroxydopamine

ISCT: International Society for Cellular Therapy

ISEV: International Society for Extracellular Vesicles

LB: Lewy Bodies

LC: Locus Coeruleus

MMPs: Matrix Metalloproteinases

MFB: Medial Forebrain Bundle

MSC: Mesenchymal Stem Cells

miRNA: microRNA

mRNA: Messenger RNA

MAP-2: Microtubule associated protein-2

MAO-B: Monoamine-oxidase B

MVB: Multivesicular bodies

Min: Minutes

NMDA: N-methyl-D-aspartate

NEP: Neprilysin

NM: Neuromelanin

ncRNA: non-coding RNA

NE: Norepinephrine

NTA: Nanoparticle Tracking Analysis

PFA: Paraformaldehyde

PD: Parkinson's disease

PNS: Peripheral Nervous System

PEDF: Pigment epithelium-derived factor

pri-miRNA: primary miRNA

RN: Raphe Nuclei

ROS: Reactive Oxygen Species

RRF: Retrorubal field

RISC: RNA induced silencing complex

RT: Room Temperature

RR: Rotarod

SCI: Spinal Cord Injury

SC: Staircase

STR: Striatum

SNpc: Substantia Nigra pars compacta

SVZ: Subventricular Zone

SPT: Sucrose Preference Test

TH: Tyrosine Hydroxylase

TEM: Transmission Electron Microscopy

UTR: Untranslated Region

VTA: Ventral Tegmental Area

WB: Western Blot

LIST OF FIGURES

LIST OF TABLES

1. INTRODUCTION

Vilaça-Faria, H., Salgado, AJ., Teixeira, FG. (2019)
Mesenchymal Stem Cells-derived Exosomes: A New Possible Therapeutic Strategy for Parkinson's Disease?
Cells, 8(2), 118
DOI: 10.3390/cells8020118

Described by James Parkinson in 1817, Parkinson's disease (PD) is the second most common chronic neurodegenerative disease in the world, affecting over 10 million people, and approximately 1% of the world population over 60 years old (Pringsheim, Jette et al. 2014). Pathologically, PD is characterized by the degeneration of dopaminergic neurons (DAn) and by the deficiency of dopamine production in several dopaminergic networks. The loss of DAn is also linked with the development/accumulation of Lewy bodies (LB; protein aggregates of α-synuclein) in the intraneuronal structure, affecting the normal functioning of those cells. From the networks impaired, the most affected one is the nigrostriatal pathway at the level of the substantia nigra pars compacta (SNpc) and the striatum (STR) (Michely, Volz et al. 2015), initially with an asymmetric onset that becomes bilateral as the disease progresses (Lees, Hardy et al. 2009). However, there are other brain areas presenting the above referred hallmarks, such as the olfactory bulb, neocortex, limbic system, and brainstem cells nuclei, suggesting a prion disease-like propagation and progression (Braak, Del Tredici et al. 2003). With this insight, an hypothesis has nowadays been proposed, supporting LB transmission among cells as a possible route for disease onset and progression. This model, called the Braak system, is divided in several stages, in which the autonomic nervous system (ANS) is the first affected by the pathology (stage 0), followed by the dorsal motor nucleus of the vagus (DMV) and the anterior olfactory nucleus (stage 1), spreading to the locus coeruleus (LC), SNpc, and basal forebrain (stage 2) and finally, to the neocortex, hippocampus, and basal ganglia (final stages) (Braak, Ghebremedhin et al. 2004). As a result, when DAn death exceeds a threshold in the nigrostriatal pathway it affects the patients' motor system. As so, PD is clinically recognized by a core of motor symptoms, including bradykinesia, rigidity, tremor, and postural instability, which are used in the establishment of its diagnosis (Anisimov 2009). However, non-motor symptoms, such as depression, sleep disorders, dementia, and peripheral impairments, have also been linked with functional disabilities, preceding the appearance of the motor symptomatology (Pantcheva, Reyes et al. 2015). Thus, the development of management strategies is crucial, in which the diagnosis and the evaluation of the condition of the patient should be accurate, being followed by the development and

application of personalized strategies, aiming to ameliorate the patient's quality of life (Teixeira, Gago et al. 2018).

1.1. Molecular and Cellular Aspects of Parkinson's Disease

As already mentioned, the major pathological feature of PD is the progressive loss of DAn in the nigrostriatal system due to the presence of intraneuronal inclusions, namely LB (Lees, Hardy et al. 2009). Along with SNpc' DAn, other neural populations of the central (CNS) and peripheral nervous systems (PNS) are affected by PD pathophysiology. For instance, in the PNS, the most affected subdivision is the ANS, in which norepinephrine (NE) neurons innervating the heart and skin (Djaldetti, Lev et al. 2009, Ghebremedhin, Del Tredici et al. 2009), as well as DAn of the enteric nervous system (ENS) (Li, Chalazonitis et al. 2011), are lost in PD. Actually, it is believed that the loss of these enteric DAn leads to orthostatic hypotension, hyperhidrosis, and constipation, some of the less explored symptoms correlated with PD development. Regarding the CNS, almost all PD patients lose its neuromelanin (NM) positive-catecholamine DAn at the levels of the SNpc and LC, something that is also observed in DMV (Halliday, Li et al. 1990). Still, DAn from the ventral tegmental area (VTA), retrorubal field (RRF), raphe nuclei (RN), and basal nucleus of Meynert (BNM) are also lost in PD, but into a lesser extent (Hirsch, Graybiel et al. 1988). Notwithstanding, although several brain regions are claimed as being affected by PD pathophysiology, only the selective loss of the SNpc' DAn recognize the core symptoms of PD. Indeed, SNpc' DAn are one of the longest and most densely arborated neurons of the brain, projecting to the STR through a long and thin unmyelinated axon (Matsuda, Furuta et al. 2009). In addition, studies have also suggested that as DAn axons make an elevated number of synaptic connections, they appear to be more prone to damage (Hindle 2010), as it has been indicated that the risk of local α-synuclein misfolding increases (Quilty, King et al. 2006). Furthermore, studies have also suggested that SNpc DAn present a pacemaker activity that is regulated by specific Ca^{2+} channels, leading to an increase in the cytosolic Ca^{2+} concentration (Michel, Hirsch et al. 2016). Such increase has been correlated with the occurrence of cellular stress, leading to the formation of reactive oxygen species (ROS), which are known to be detrimental to DAn viability (Puspita, Chung et al. 2017). The mitochondria is responsible for the DAn calcium homeostasis, which in turn increases energy demand, contributing to the vulnerability of these neurons (Surmeier, Guzman et al. 2011). In addition to this, dopamine itself could also be detrimental to DAn vulnerability, as studies have demonstrated that the increase of free cytosolic dopamine caused by an unbalanced homeostasis at several levels (synthesis, storage, degradation, and/or distribution in the

synaptic vesicles) favors ROS production and oxidative stress, leading to DAn damage (Asanuma, Miyazaki et al. 2003, Juarez Olguin, Calderon Guzman et al. 2016). Moreover, the SNpc' DAn present a dark colored pigment, NM, which acts as a reservoir of iron, metals, and other toxic substances, having a neuroprotective effect (Haining and Achat-Mendes 2017). In addition to neuroprotection, NM has recently been proposed as a promising biomarker for PD, although such hypothesis remains to be proved (Sulzer, Cassidy et al. 2018). On the other hand, (DAn) dying neurons release NM to the extracellular space, creating deposits that induce microglial activation, chemotaxis, and proliferation, thus supporting SNpc inflammation and neuronal degeneration (Zhang, Phillips et al. 2011). These multifactorial features led to the study of the underlying mechanisms responsible for the loss of DAn linked to PD.

Rationally, the first question to be answered is how does PD begin at the cellular level? Although this answer remains under discussion, several studies have demonstrated that the degeneration in PD initiates in the synaptic and axonal terminals, beginning in the STR, and in a retrograde manner, progresses to the SNpc' DAn somas (Hornykiewicz 1998). In fact, the literature shows that, at the time of the motor symptoms onset, 30% of the SNpc' DAn are lost, while 50–60% of the axon terminals in the STR are already degenerated (Cheng, Ulane et al. 2010). However, the exact mechanisms of such degeneration are still not understood and some concepts have been proposed throughout time. The most relevant mechanisms involving PD include the disruption of protein clearance pathways, the accumulation of α-synuclein protein aggregates, mitochondrial dysfunction, glutamate/calcium excitotoxicity, oxidative stress, neuroinflammation, and genetic mutations (Dexter and Jenner 2013). Most of these mechanisms are related to DAn sensitivity and susceptibility to degeneration, as previously described. However, cell death may be caused by specific genetic mutations, which in turn affect several PD interlayers. Pathogenic mutations in PD can lead to protein degradation systems' (ubiquitin-proteasome and autophagy-lysosome system) failure, which leads to the accumulation of misfolded α-synuclein, defective mitochondria, thereby creating intercellular oxidative stress, and thus leading to DAn degeneration (Komatsu, Waguri et al. 2006, Chu, Dodiya et al. 2009). Although it represents less than 10% of all PD cases, at least 17 autosomal dominant and autosomal recessive gene mutations, namely, α-SYN (SNCA), PARKIN (PRKN), ubiquitin C-terminal hydrolase L1 (UCHL-1), PTEN-induced putative kinase 1 (PINK1), protein deglycase (DJ-1, PARK7), and leucine-rich repeat kinase 2 (LRRK2, PARK8) genes, among others have been identified (Dexter and Jenner 2013). Notwithstanding, although most of the PD cases are sporadic (idiopathic), being caused by an interaction between genetic and environmental factors (Warner and Schapira 2003), such as aging, inflammation, and exposure to neurotoxic agents (e.g., pesticides, such as rotenone and paraquat), both sporadic and familial forms of PD have mutual molecular pathways, as

shown in Table 1, making PD a multi-targeted disease in which new strategies, with a multimodal action, may be of particular value (Hirsch, Jenner et al. 2013).

Table 1. Sporadic and genetic types of Parkinson's Disease (PD).

SPORADIC PD	
• **Disruption of protein clearance pathways** • **Accumulation of α-synuclein protein** • **Mitochondrial dysfunction** • **Excitotoxicity** • **Oxidative stress** • **Neuroinflammation**	
GENETIC PD	
SNCA	Accumulation of α-synuclein protein aggregates.
PRKN	Decrease in DJ-1 and PARKIN proteins, which leads to mitochondria dysfunction when in oxidative stress conditions.
PARK7	
UCHL-1	No stabilization of ubiquitin monomers, which can lead to ubiquitin-proteasome system dysfunction.
PINK1	Reduction in PTEN induced putative kinase 1 activity, which can lead to mitochondria malfunction.
PARK8	Overexpression of LRRK2 that causes DAn loss, accompanied by the presence of LB.

1.2. Parkinson's Disease Treatments: Do We Have What is Needed?

The loss of DAn and reduced dopamine production underlies the reasoning of the PD gold standard treatment, which is still the administration of levodopa (Cotzias, Van Woert et al. 1967, Hornykiewicz 2015). However, this strategy remains insufficient to recover lost DAn, or to avoid PD progression, as its extended use, associated with the needs of increased dosages, is linked with secondary effects, such as motor fluctuations and behavioral changes (e.g., impulsivity and addiction) (Singh, Pillay et al. 2007). The field's current view is that combinatory strategies may overcome the limitations of single levodopa administration, particularly by combining the latter with other PD pharmacological treatments. Such combined treatments have demonstrated the ability to enhance and prolong levodopa efficacy by involving

the use of dopamine receptor agonists (e.g., ropinirole, pramipexole, piribedil) (Im, Ha et al. 2003); inhibitors of peripheral enzymes, such as levodopa decarboxylase (e.g., carbidopa and benserazide) (Rinne and Molsa 1979) or catechol-O-methyl transferase (COMT) (e.g., entacapone, tolcapone, and, more recently, opicapone) (Lees 2008, Fabbri, Ferreira et al. 2018); and inhibitors of central enzymes, such as monoamine-oxidase B (MAO-B) (e.g., selegiline, rasagiline, or safinamide) (Dezsi and Vecsei 2017, Teixeira, Gago et al. 2018) for oral intake. Besides these, throughout the years, other options were developed without the direct application of levodopa. This includes other dopamine agonists, such as rotigotine by transdermal application (Zhou, Li et al. 2013), and apomorphine by subcutaneous administration (Boyle and Ondo 2015). Also, then N-methyl-D-aspartate (NMDA) receptor antagonist (e.g., amantadine) was found to improve PD motor impairments, by reducing dyskinesia and other PD-related complications (Kong, Ba et al. 2017). Surgical procedures, such as deep brain stimulation (DBS), have also been used in the treatment of PD, being a procedure that comprises the delivery of electrical pulses to neurons through a neurostimulator implantation, either in the subthalamic nucleus or in the internal part of the globus pallidus, leading to symptomatic relief (Groiss, Wojtecki et al. 2009).

In addition to these pharmacological and surgical treatments, in the last years, a large number of new approaches have been developed to verify the effect of molecular agents (e.g., adenosine receptor antagonists, anti-apoptotic agents, and antioxidants) and non-pharmacotherapies (e.g., viral vector gene therapy, microRNAs, transglutaminases, and RTP801) in the treatment of PD (Tarazi, Sahli et al. 2014). However, although promising results have been experimentally and clinically obtained with several drugs and surgical experiments, yet the challenge remains to show a clinical proof of arrest of delay of DAn loss in PD (Teixeira, Gago et al. 2018). Therefore, there is an urgent need for the establishment of innovative therapies that adequately target PD, particularly by inducing neuroprotection of the surviving DAn within the SNpc-STR pathway, as well as stimulating the differentiation of new ones, so that the dopamine balance can be re-established. With the advent of stem cell biotechnology, new routes are currently being explored, particularly those aiming to protect DAn, as it is the case of human mesenchymal stem cells (MSCs)-derived exosomes (Marote, Teixeira et al. 2016, Keshtkar, Azarpira et al. 2018). Therefore, in the scope of this review, we will discuss the current understanding of MSCs-derived exosomes by reviewing recent experimental data addressing the therapeutical potential of those vesicles in the context of PD.

1.3. Mesenchymal Stem Cells (MSCs) Secretome and Parkinson's Disease

As we have previously reviewed, according to the definition introduced by the International Society for Cellular Therapy (ISCT), there are some minimal criteria for the identification of MSCs populations, namely 1) the adherence to plastic in standard culture conditions; 2) the positive expression of specific markers, like CD73, CD90, and CD105, and negative expression of hematopoietic markers, like CD34, CD45, HLA-DR, and CD14, or CD11B, CD79α, or CD19; and 3) *in vitro* differentiation into at least osteoblasts, adipocytes, and chondroblasts (Dominici, Le Blanc et al. 2006, Teixeira, Carvalho et al. 2013). Therefore, MSCs are a multipotent non-hematopoietic stem cell population that has emerged in the last decade as a promising therapeutic tool for the treatment of several disorders, including PD (Teixeira, Carvalho et al. 2013, Marote, Teixeira et al. 2016). This potential is associated with their widespread availability throughout the human body, namely in the bone marrow, adipose tissue, brain, dental pulp, placenta, umbilical cord blood, and Wharton's jelly (Teixeira, Carvalho et al. 2013, Salgado, Sousa et al. 2015). Notwithstanding, it is important to highlight that although all these populations are within the definition of MSCs, they can have subtle differences, mainly in their membrane antigen markers (Teixeira, Carvalho et al. 2013). Indeed, studies have demonstrated that such differences may be the result of different cell culture protocols in their isolation and expansion or, alternatively, be related with the tissue source from which they are being isolated (Chamberlain, Fox et al. 2007, Phinney 2007). Although, from the application point of view, studies have shown that after (intracranial) transplantation, these cells act as promoters of immunomodulation, neuroprotection, and neuronal differentiation (Teixeira, Carvalho et al. 2015, Gao, Chiu et al. 2016). These effects are essentially mediated by the products that are released by MSCs into the extracellular milieu, commonly defined as secretome (Joyce, Annett et al. 2010). MSCs-secretome has been described as a complex mixture of soluble products composed by a proteic soluble fraction (constituted by growth factors and cytokines), and a vesicular fraction composed by microvesicles and exosomes, which are involved in the transference of proteins and genetic material (e.g., miRNA) to other cells, with promising therapeutic effects (Teixeira, Carvalho et al. 2013, Marote, Teixeira et al. 2016).

Our lab has shown that MSCs-secretome acts as an important promoter of neuroprotection, and neurodifferentiation, by modulating neural stem cells, neurons and glial cells, and axonal growth *in vitro* and *in vivo* environments (Salgado, Fraga et al. 2010, Ribeiro, Salgado et al. 2011, Ribeiro, Fraga et al. 2012, Fraga, Silva et al. 2013, Teixeira, Carvalho et al. 2015, Martins, Costa et al. 2017, Assuncao-Silva, Mendes-Pinheiro et al. 2018, Serra, Costa et al. 2018). More recently, we have revealed that the use of dynamic culturing conditions (through computer-controlled bioreactors) can further modulate MSCs-

secretome, generating a more potent neurotrophic factor cocktail (Teixeira, Panchalingam et al. 2015, Teixeira, Panchalingam et al. 2016). In the context of PD, we have recently shown that its administration in the SNpc-STR pathway was able to partially revert the motor and histological symptoms of a 6-OHDA rat model of PD (Teixeira, Carvalho et al. 2017), indicating that MSCs-secretome can be used as a therapy. Following on this work we have identified the presence of important neuroregulatory molecules in the secretome of MSCs, including BDNF, IGF-1, VEGF, Pigment epithelium-derived factor (PEDF), DJ-1, and Cystatin-C (Cys-C), that are being described as potential therapeutic mediators against PD [62,65], as well as matrix metalloproteinases (MMPs), namely MMP 2, known for being able to degrade α-synuclein aggregates (Pires, Mendes-Pinheiro et al. 2016, Oh, Kim et al. 2017), and have correlated their presence with the impact observed in our *in vitro* and *in vivo* models.

In addition to this protein fraction, the secretome also presents a vesicular portion, which is composed by extracellular vesicles (EVs). The latter are important in cell-to-cell communication, as they are involved in the transference of proteins and genetic material to neighboring cells (Qin and Xu 2014). EVs are secreted by different cell types, such as neurons, microglia, epithelial, endothelial, and hematopoietic cells, and stem cells as MSCs (Budnik, Ruiz-Canada et al. 2016). According to the International Society for Extracellular Vesicles (ISEV), EVs are characterized by three minimal criteria: (1) Isolation from conditioned cell culture medium or body fluids, with negligible cell disruption; (2) quantification of one protein (at least) from three distinctive categories in the EV preparation - cytosolic proteins, transmembrane or lipid bound extracellular proteins, and intracellular proteins; and (3) vesicles characterization using at least two different technologies—by imaging (e.g., electron microscopy or atomic force microscopy) and EVs size distribution measurements (e.g., nanoparticle-tracking analysis or resistive pulse sensing) (Lotvall, Hill et al. 2014). EVs are classified as microvesicles, exosomes, and apoptotic cell bodies (Beer, Mildner et al. 2017) based on their size, origin, and cargo. Regarding their size, exosomes are the smallest type, being classified as vesicles with a range of 30-150 nm, while microvesicles and apoptotic bodies have 50–1000 nm and 50–2000 nm in diameter, respectively (Lener, Gimona et al. 2015). EVs are distinguished as exosomes if formed inside multivesicular bodies (MVBs) at the endolysosomal pathway and secreted upon MVBs fusion with the membrane, in contrast to microvesicles, which form from the sprouting of the plasma membrane, while apoptotic bodies originate from dying cells fragments (Stephen, Bravo et al. 2016). Exosomes are the best characterized EV population and were first discovered in 1983 in maturing sheep retilocytes (Harding and Stahl 1983). Exosomes present a phospholipid layer characterized by sphingolipids, ceramides, tetraspanins (CD63, CD9, CD81), fusion proteins (flotillins, CD9, annexin), integrins, heat shock proteins (HSC70 and HSC90),

membrane transporters (GTPases), lysosomal proteins (Lamp2b), tumor sensitive gene (TSG101), and Alix (Mathivanan, Ji et al. 2010). Regarding their cargo, exosomes contain a variety of biomolecules, such as cell-type specific proteins, signaling peptides, lipids, and genetic material (e.g., miRNA, small RNA, genomic DNA, mRNA, long non-coding RNA, tRNA, cDNA, and mtDNA), which once released to the extracellular environment, are taken up by other cells (McKelvey, Powell et al. 2015). This interaction can lead to changes in the cell phenotype or to a modulation of the cell activity, raising the question of whether exosomes can represent the basis for the creation of new therapeutical strategies under the (CNS) regenerative medicine field. Indeed, studies have remarkably explored and demonstrated exosomes as a delivery system of therapeutical signals or drugs due to their low immunogenicity, ability to cross the blood-brain barrier (BBB), and long half-life in circulation (Kalani, Tyagi et al. 2014). As described, different cell types secrete exosomes, however, in this review, we highlight the ones derived from the secretome of MSCs, since they show promising effects by triggering regenerative responses in different pathological conditions. MSCs-derived exosomes were firstly isolated and described in 2010 from human MSCs-derived from embryonic stem cells (ESC) (Lai, Arslan et al. 2010). Actually, since their discovery, an increasing number of studies explored their regenerative potential using diverse *in vitro* and *in vivo* models of several pathological conditions by demonstrating that the uptake of MSCs-derived exosomes is able to stimulate angiogenesis and myogenesis, promote functional and morphologic rescue due to a decrease of oxidative stress and suppression of apoptosis, as well as the modulation of inflammatory responses (Arslan, Lai et al. 2013, Zhou, Xu et al. 2013, Bian, Zhang et al. 2014, Tan, Lai et al. 2014, Zhang, Yin et al. 2014, Nakamura, Miyaki et al. 2015).

Concerning CNS pathologies, MSCs-derived exosomes have also shown therapeutical benefits. For instance, in stroke, intravenous administration of MSCs-derived exosomes induced an increase of neurogenesis, neurite remodeling, and angiogenesis, facts that were correlated with a substantial improvement of animals' functional recovery (Xin, Li et al. 2013). Such a tendency was also observed in a traumatic brain injury model, showing an inflammation reduction and good outcomes after MSCs-derived exosomes' administration (Zhang, Chopp et al. 2015). The injection of MSCs-derived exosomes has also been shown to be a possible treatment for spinal cord injury (SCI), by reducing inflammation and by promoting neuro-regeneration in rats after injury (Han, Wu et al. 2015, de Rivero Vaccari, Brand et al. 2016). In neurodegenerative diseases, such as Alzheimer's, studies have shown MSCs-derived exosomes expressing high levels of the amyloid β-degrading enzyme, neprilysin (NEP), leading to a decrease of brain Aβ levels (Katsuda, Tsuchiya et al. 2013), and thus having an impact on the disease progression. In the context of PD, MSCs-derived exosomes were found to rescue DAn in *in vitro* (6-OHDA)

models of PD, providing a potential regenerative treatment for this disorder (Jarmalaviciute, Tunaitis et al. 2015).

However, although promising results have been claimed by MSCs-derived exosomes, studies have also claimed that the exosomes content depends on the tissues where MSCs are originally isolated and the environment in which they are present, setting the need to further study the different functional exosomal properties. Such assumption is in line with previous results published by our group, which demonstrated that MSCs from different sources have different secretome profiles, thereby indicating that such a difference in their secretion pattern may indicate that their secretome or derived vesicles may be specific to a condition of the CNS (Pires, Mendes-Pinheiro et al. 2016).

1.4. Exosomal Genetic Material Content: Are miRNAs Important in the Modulation of the Molecular and Cellular Issues of PD?

As previously mentioned, one of the most common content of exosomes is the presence of genetic material, such as microRNAs (miRNAs) (Gong, Yu et al. 2017). Actually, it has been indicated that numerous diseases, including PD, exhibit intense dysregulation of gene expression, specifically at the miRNA level (Sonntag 2010) — Figure 1. In addition to its involvement in PD pathophysiology, exosome-derived microRNAs have also been identified as a potential tool for diagnosis biomarkers and targeted therapies.

miRNAs are the most studied class of non-coding RNAs (ncRNA), with between 21–25 nt, and are responsible for the regulation of specific genes through messenger RNA (mRNA) degradation or inhibition of their translation (Krol, Loedige et al. 2010). Still, miRNAs bind to the untranslated region (UTR) of the mRNA target and recruit the RNA induced silencing complex (RISC) in order to inhibit the expression of these targets, therefore, regulating specific gene expression, and presenting key roles in normal cellular physiology (Brodersen and Voinnet 2009). In animals, miRNAs are produced in two stages, starting from primary miRNAs (pri-miRNAs), and by the action of Drosha/DGCR8 RNase in the nucleus, and Dicer RNase in the cell cytoplasm (Wahid, Shehzad et al. 2010). This miRNA biogenesis pathway is of great importance and is essential for normal development since Dicer knockout mice are not able to survive beyond the embryonic stage (Bernstein, Kim et al. 2003). Also, it was shown that impairments in Dicer in mice midbrain leads to a progressive loss of DAn (Pang, Hogan et al. 2014), and post-mortem brain analysis showed DAn loss combined with LB, when the DGCR8 gene was deleted (chromosome 22q11.2 deletion syndrome) (Butcher, Kiehl et al. 2013).

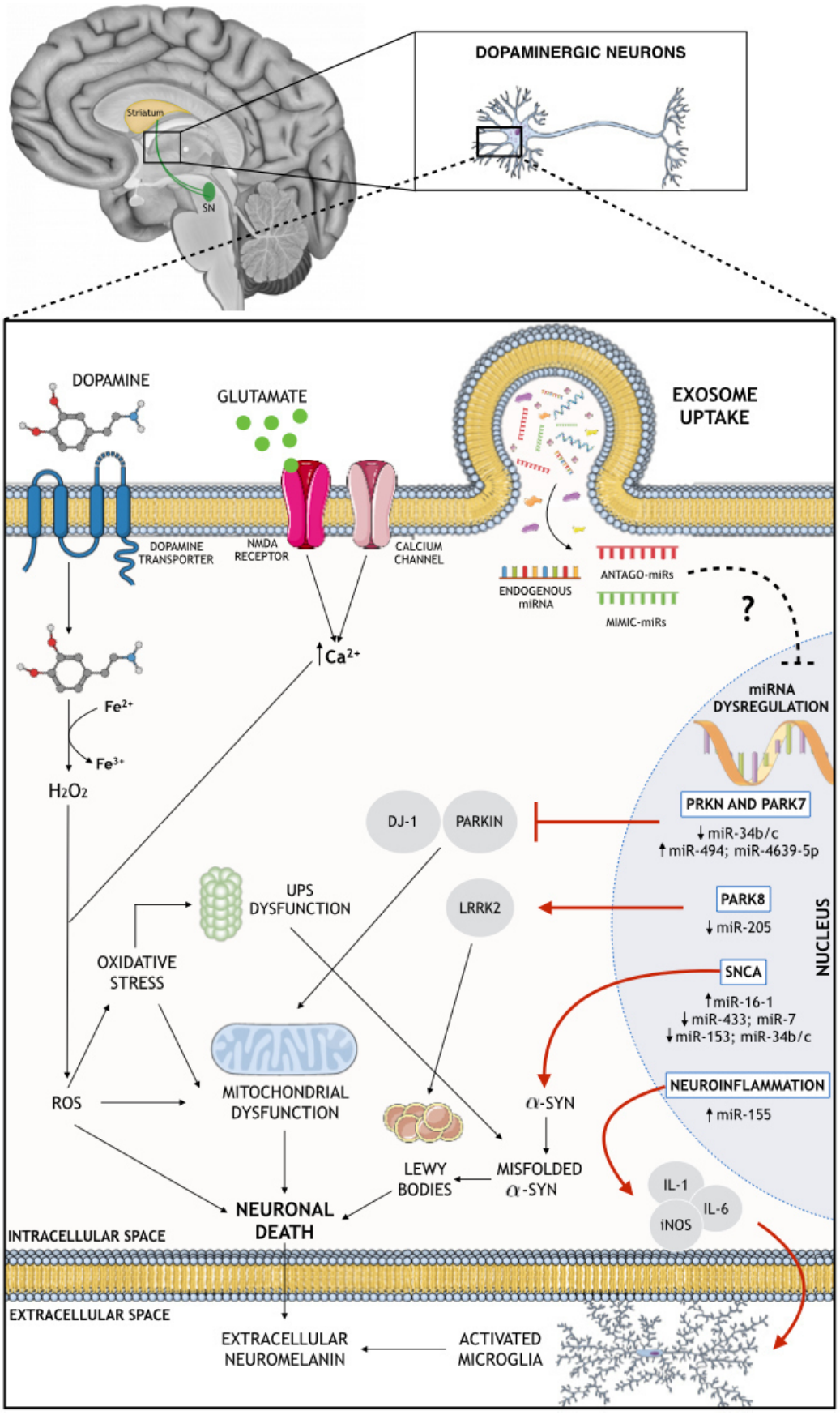

Figure 1. Schematic representation of the role of miRNAs in the molecular and cellular (e.g. nuclear, intracellular, and extracellular) mechanisms of PD brain.

Several miRNA-mediated dysfunction networks in PD-related genes have recently been reported. Concerning the SNCA gene, several miRNAs have been suggested as α-synuclein modulators. For instance, interference in the binding between miR-433 and fibroblast growth factor 20 (FGF20) mRNA leads to increased levels of FGF20, which in turn also increases the levels of the α-synuclein protein in the cell (Wang, van der Walt et al. 2008). Moreover, an abnormal increase of the miR-16-1 levels inhibits to a greater extent the translation of the HSP70 mRNA (protein that inhibits α-synuclein), which in turn also leads to an increase of the α-synuclein protein levels (Zhang and Cheng 2014). Also, PD-related pathogenic processes blocking miR-7, miR-153, and miR-34b/c from binding on their α-synuclein mRNA target automatically leads to increased levels of α-synuclein (Doxakis 2010, Fragkouli and Doxakis 2014, Kabaria, Choi et al. 2015). Regarding PRKN and PARK7 genes, they express, respectively, the PARKIN and DJ-1 proteins, which present important roles in the normal cell functioning and PD. PARKIN protein partakes in the proteasome-mediated degradation, and it is expressed in the mitochondria, where it binds to mtDNA, protecting it against damage promoted by oxidative stress conditions (Rothfuss, Fischer et al. 2009). DJ-1 protein is considered an oxidative detector and it binds to PARKIN protein in oxidative stress conditions, protecting the mitochondria from oxidative stress (Moore, Zhang et al. 2005). Also, mutations in the PARK7 gene make DAn more susceptible to ROS-mediated damage (Billia, Hauck et al. 2013) . In PD, a correlation was found between the decrease of miR-34b/c levels and the consequent decrease of the PARKIN and DJ-1 proteins in several brain areas (Minones-Moyano, Porta et al. 2011). Also, an upregulation of miR-494 and miR-4639-5p causes a direct reduction of DJ-1 protein expression, making DAn more vulnerable and prone to PD phenotype (Xiong, Wang et al. 2014, Chen, Gao et al. 2017). Moreover, LRRK2 gene (PARK8) mutations cause sporadic PD associated to a neuropathology characterized by SNpc' DAn loss, which is, in some cases, accompanied by the formation and presence of LB (Santpere and Ferrer 2009). In fact, studies verified an increase of LRRK2 expression in PD patients when compared with controls, correlating this increase with a downregulation of miR-205 (Cho, Liu et al. 2013). Another miRNA associated with the dopaminergic phenotype in PD is miR-133b, which is found to be downregulated in PD patients, and it regulates the transcriptional activator, Pitx3, an important factor in DAn development (Kim, Inoue et al. 2007). Additionally, other miRNAs were found to regulate the expression of genes involved in neuroinflammation, an important hallmark of PD. In this context, studies have found that miR-155 plays a key role in the upregulation of the inflammatory response to α-synuclein fibrils. This occurs by the fact that miR-155 is a modulator of proinflammatory molecules, such as IL-1, IL-6, TNF-α, and iNOS, leading to its upregulation (Ponomarev, Veremeyko et al. 2013). Also, an miR-155 knockout mice model showed that the lack of this miRNA prevented reactive microgliosis, as

well as the loss of DAn triggered by the overexpression of α-synuclein (Thome, Harms et al. 2016). In the same line of thought, miR-7, which was previously reported as an important factor in the regulation of α-synuclein levels, has also been presented as an important player in the modulation of neuroinflammation. For instance, the injection of miR-7 in the STR of an MPTP mouse model of PD was found to block NLRP3 inflammasome activation, leading to a remarkable attenuation of DAn death (Zhou, Lu et al. 2016).

In addition to this involvement in PD pathophysiology, miRNAs are also being investigated as a potential source of PD biomarkers, in which the exosomes are being identified as a great use for diagnosis and prognosis of the disease. Indeed, Vizoso and colleagues (Vizoso, Eiro et al. 2017) have recently proposed that MSCs-derived secretome is sufficient to significantly improve multiple biomarkers of the pathophysiology, making it a potential strategy to be used for the establishment and identification of promising PD biomarkers. As we have previously described, MSCs are able to secrete large quantities of exosomes carrying miRNAs, and such miRNAs may function not only as a novel class of promising biomarkers, but as modulators of multiple systems that could play critical roles in several diseases, including PD. Therefore, the possibility of using it as a potential therapeutic strategy for the treatment of PD is starting to emerge. To target the brain areas affected in PD, miRNAs must be delivered into the brain through a transport system able to cross the BBB—Figure 2. Due to the multi-faceted nature of exosomes, its application in clinics is something that could be envisaged in the near future (Ha, Yang et al. 2016). However, firstly, some challenges need to be addressed, namely: 1) The correct (MSC) cell line; 2) exploration of the most efficient and reliable yield isolation technique associated to an efficient scalable production; 3) development of robust loading methods without damage to the exosomal integrity, in order to ensure an improved insight into PD cellular and molecular mechanisms, and finally to 4) address and plan possible strategies to improve (MSCs) exosomes' targeting capability. MSCs-derived exosomes may constitute a new key solution. Indeed, several studies show that MSCs-derived exosomes are able to transfer miRNAs to neuronal cells, in which exosomes enriched in miR-133b can promote neurite outgrowth (Xin, Li et al. 2012), which is of great benefit for PD, as it is one of the miRNAs that is normally downregulated in the disease. Still, miR-143 and miR-21 were also found to be present in MSCs-derived exosomes, being described as important players in immune response modulation and in neuronal death associated with an environment of chronic inflammation (Baglio, Rooijers et al. 2015). Similarly, a miRNA cluster is also present in MSCs-derived exosomes, being formed by miR-17, miR-18a, miR-19a/b, miR-20a, and miR-90a, and being described as important modulators of neurite remodeling and neurogenesis, as well as stimulators of axonal growth and CNS recovery (Xin, Katakowski et al. 2017).

For instance, mimics, such as mimic-miR-124, are able to promote subventricular zone (SVZ) neurogenesis, which was shown after intracerebral administration in a 6-OHDA mice model of PD, and was also correlated with significant behavioral improvements (Saraiva, Paiva et al. 2016). In contrast, the mimic-miR-7 is able to suppress NLRP3 and α-synuclein in the nigrostriatal pathway, thereby providing a potential therapeutic effect for PD. Regarding the antago-miRs, the antago-miR-155 may be relevant to PD therapy, since miR-155 plays a key role in the microglial cells activation in PD, leading to neuroinflammation.

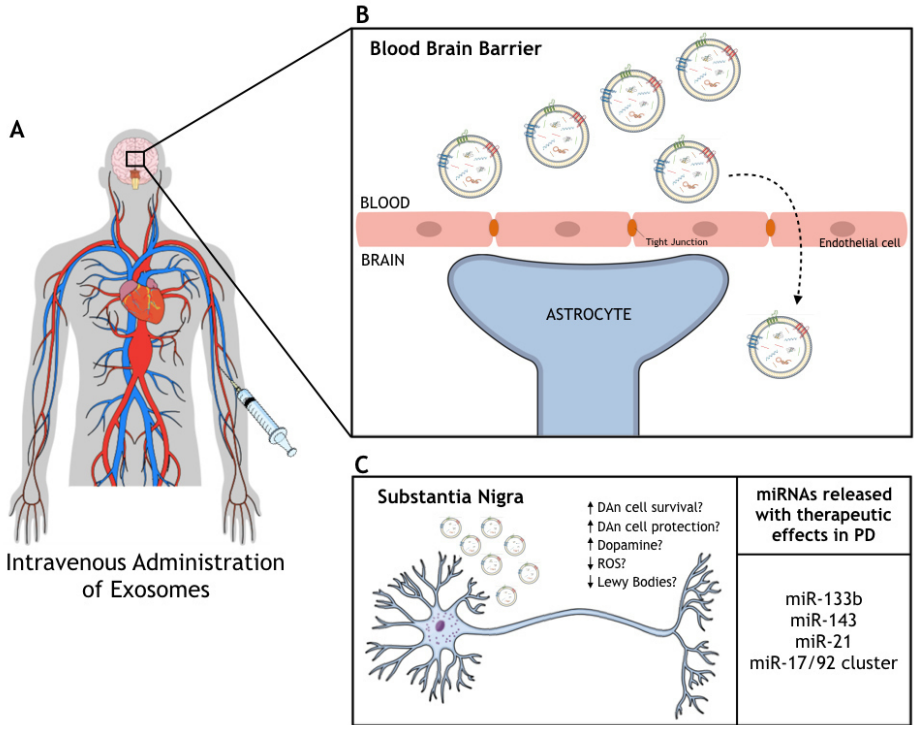

Figure 2. Schematic representation of the active role of exosomes on PD. How exosomes recognize and internalize other cells remains under discussion. Free-floating, adhesion, and antigen recognition have been described as mechanisms of cellular recognition, while soluble and juxtacrine signaling, fusion, phagocytosis, micropinocytosis, and receptor- and raft-mediated endocytosis have been described as mechanisms of exosomal internalization, as described by (McKelvey, Powell et al. 2015).

Finally, the overexpression of miR-126 leads to an impairment in the IGF-1 signaling, increasing DAn vulnerability to the PD neurotoxin, 6-hydroxydopamine (6-OHDA). Notwithstanding, when using an antago-miR-126, the opposite occurs, resulting in neuroprotective effects induced by IGF-1 (Kim, Lee et al. 2014). In summary, the development of an understanding of the molecular mechanisms regulated by miRNAs and the potential of MSCs-derived exosomes in how they impact PD brain homeostasis may allow the creation and development of important clinical gains to be translated to PD patients.

2. RESEARCH OBJECTIVES

Satisfactory approaches to relief/slow down PD by protecting DAn from premature death are still missing and, although several strategies have showed promising results, yet remains the challenge to show proof of arrest of delay of DAn loss in PD (Teixeira, Gago et al. 2018). MSCs secretome has been on the forefront of a new wave of possible therapeutic strategies for CNS regeneration. This is extremely important as, instead of transplanting cells, one could envisage therapies where just the secretome of stem cells could be used. Indeed, MSCs secretome has been described as a complex mixture of soluble products composed by a protein soluble fraction (constituted by growth factors and cytokines), and a vesicular fraction composed by extracellular vesicles (as exosomes) with promising therapeutic effects (Baglio, Pegtel et al. 2012, Drago, Cossetti et al. 2013, Salgado and Gimble 2013, Teixeira, Carvalho et al. 2013, Marote, Teixeira et al. 2016). Although our lab has recently identified promising molecules with neuroregulatory potential on MSCs secretome (Teixeira, Carvalho et al. 2013), the identity of all therapeutic molecules on it remains a challenge. Moreover, as far as we know there are no studies addressing the impact of the different secretome fractions. Therefore, on the scope of the present thesis our objectives were:

1. Isolate, and purify human bone marrow MSCs (hBM-MSCs) secretome-derived exosomes through ultracentrifugation procedures.
2. Address the impact of hBM-MSCs secretome-derived exosomes on neuronal survival and differentiation on human neural progenitor cells (hNPCs) and in *in vitro* models of PD.
3. Assess the impact of hBM-MSCs secretome-derived exosomes in an *in vivo* 6-hydroxydopamine (6-OHDA) rat model of PD.

3. MATERIALS AND METHODS

3.1. Cell Culture

3.1.1. Expansion of hBM-MSCs and Secretome Collection

Human bone marrow-derived mesenchymal stem cells (hBM-MSCs) pre-isolated and cryopreserved were thawed at 37°C and plated in T-75 – treated polystyrene flask culture with 15 mL of α-MEM growth medium [(α-MEM, NaHCO3, 1% Pen-Strep and 10% FBS-exosome free (overnight ultracentrifugation of FBS at 120.000 x g)]. The cell culture was maintained in an incubator at 37°C, 5% CO_2 and the medium was renewed every 2 days. After 80-90% of cell confluency, the cells were enzymatically digested with 0.05% trypsin during 5 minutes (min) at 37°C. The cell culture growth medium was used to stop the reaction. Following that, the cells were centrifuged at 1.200 rpm for 5 min, the pellet was resuspended and using a Neubauer chamber, the trypan blue method was used to perform cell counts. 5 x 10^5 cells were plated into new cell culture flasks and the procedure was repeated until cells reach passage 5 (P5). At P5 (12.000 cells/cm^2), and after 3 days of cell growth, the medium was removed and the cells were washed 3 times with PBS 1x (without Mg^{2+} and Ca^{2+}) and 3 times with Neurobasal A medium. Following this, the hBM-MSCs culture was incubated with Neurobasal A supplemented with 1% kanamycin. After 24h, the secretome was collected and stored at 4°C or -80°C until usage.

3.1.2. Expansion of hNPCs

Human neural progenitor cells (hNPCs) were obtained from Prof. Leo A. Behie's lab (University of Calgary, Canada) and were isolated from the telencephalon region of a 10-week-old fetus in agreement of the parental entities and according with the protocols and ethical guidelines established by the Conjoint Health Research Ethics Board (University of Calgary, Canada; ID: E-18786) (Baghbaderani, Mukhida et al. 2010). hNPCs pre-isolated and cryopreserved were thawed at 37°C and placed in T-75 culture flasks with 15 mL of PPRF-h2 serum-free medium and maintained in an incubator at 37°C, 5% CO_2. After 2-4 days of growth in culture, the cells were submitted to a mechanical dissociation process. This consists on the cells' centrifugation for 10 min at 1000 rpm followed by trituration using a P1000 set to 850 μL (25-35 times). This turns the previous hNPCs aggregates into a single cell suspension, being then cultured in fresh PPRF-h2 growth medium, and having into account the cell density of 100.000 cells/mL. Every 2 days, 40% of the growth medium was replaced with fresh growth medium and the culture was maintained at 37°C in an incubator with 5% CO_2. After 14-20 days of growth, hNPCs were centrifuged at 1000

rpm for 10 min and then dissociated enzymatically using 0.05% Trypsin (1 mL) during 3 min at 37°C. To stop trypsin activity, 5 mL of growth medium was added to the cell suspension, followed by an ultracentrifugation of 1000 rpm for 10 min. The supernatant was discarded, and the cells pellet resuspended in 1 mL of growth medium, enduring 25-35 times of trituration, as previously described in the mechanical dissociation process. The subsequent single cell suspension was then used to perform cell counts, through the trypan blue method. Finally, the cells were plated into new culture flasks at a density of 100.000 cells/mL.

3.1.3. Dopaminergic Neurons (DAn) – derived from mouse Embryonic Stem Cells Generation

The formation of DAn – derived from mouse Embryonic Stem Cells (mESCs) was comprised in 3 stages: Expansion of undifferentiated mESCs, Embryoid Bodies (EBs) generation, and DAn differentiation. Firstly, a specific undifferentiated TH-GFP mESCs cell line (Chumarina, Azevedo et al. 2017) was maintained on an immortalized mouse embryonic fibroblasts (mEF) feeder layer in a ES cell medium (DMEM Glutamax, 10% FBS, L-Glutamine, 1% Non-essential amino acids (NEAA), 1% Pen/Strep, 1% Nucleosides, and beta-mercaptoetanol (BME)), with supplementation with LIF factor. The cell culture was kept in an incubator at 37°C, 5% CO_2 and the medium was renewed every other day. This process was maintained until cells reached confluency, in which an enzymatic digestion protocol was carried as previously described. This is associated with the beginning of the EBs formation phase, in which, cells are plated in a low-attachment cell culture flask with a ADFNK differentiation medium (Advanced DMEM:F12 + Neurobasal, 10% Knockout Serum Replacement (KSR), L-Glutamine, BME). After 2 days, the ADFNK medium was supplemented with specific factors (SAG) and was changed and supplemented every day. On day 10, the ADFNK medium was supplemented with additional factors such as BDNF, GDNF, and ascorbic acid, initiating the last phase of the process (DAn differentiation). This final ADFNK medium was replaced every day for 14 days, allowing the DAn differentiation to occur. On day 14, collagen hydrogel droplets (rat tail collagen type I (3.61 mg/mL; 89.6% [vol/vol]; BD Biosciences, USA), DMEM 10x, NaHCO3) were used as described in (Gomes, Mendes et al. 2018) as a supportive matrix for EBs adhesion and growth. EBs were collected and placed individually on top of the collagen droplets with their normal growth medium (ADFNK medium). EBs were kept in culture for 6 days and media was changed every day. After 6 days, cells were insulted with 6-OHDA and treated with hBM-MSCs secretome different fractions, assessing cells viability.

3.2. Isolation of hBM-MSCs Secretome – derived Exosomes

hBM-MSCs secretome was collected from approximately 6 x 10^6 cells at P5. Exosomes were isolated as described in (Cunha, Gomes et al. 2016). Briefly, hBM-MSCs secretome was submitted to a set of differential centrifugations all performed at 4°C, in which the initial one (1.000 x g for 1 hour) aimed to remove the cells, dead cells and cell debris existent in the medium. The supernatant was then transferred to Ultra-Clear tubes and centrifuged at 16.000 x g for 1 hour in a JA-25.50 fixed-angle rotor (Beckman Coulter Inc., USA) to pellet high size range microvesicles. The remaining supernatant is filtered in a 0.22 μm pore filter (Sarstedt, Germany) to remove particles larger than 200 nm and then transferred to Polycarbonate with CAP Ultra-Clear Tubes (10.4 mL, 355603, Beckman Coulter Inc., USA) and centrifuged at 100.000 x g for 2 hours in a 90 Ti fixed-angle rotor (Beckman Coulter Inc., USA) to pellet exosomes. The exosome-containing pellet was resuspended in PBS and centrifuged again at 100.000 x g for 2 hours to remove any contaminating proteins. The pellet was then resuspended in 50-100 μl of appropriate buffer (PBS for DLS analysis and Neurobasal A medium for the *in vitro* assays) and stored at 4ªC to be used immediately or at -80°C until usage.

3.3. hBM-MSCs Secretome-derived Exosomes Characterization

3.3.1. Dynamic Light Scattering (DLS)

Exosomes previously isolated from the secretome of hBM-MSCs were diluted in approximately 900 μl of PBS and further analyzed by Dynamic Light Scattering (DLS) (633 nm wavelength laser) using a Zetasizer Nano ZS (Malvern Instruments, Holand) for size distribution of the sample. The DLS measurements of the sample were performed at a 90° angle and undertaken in sextuplicates at room temperature (RT).

3.4. *In vitro* Assay

3.4.1. Growth and Incubation of hNPCs with hBM-MSCs secretome separated fractions

Followed by the mechanical and enzymatic dissociation previously described, hNPCs were left in culture to expand. After 10-15 days of growth, hNPCs were submitted to an enzymatic dissociation in order to turn them into a single cell suspension, and were plated into a pre-coated [poly-D-lysine (100 μg/mL, Sigma, USA) for 90 min and laminin (10 μg/mL, Sigma, USA) for 3 hours] 24-well plate at a density of 100.000 cells/well. The cells were incubated with 5 different conditions, namely: CT^+- Positive control that comprises the optimal cell differentiation medium, CT^- —Negative control that contains only Neurobasal A medium with 1% of kanamycin, CM – Internal positive control that contains MSCs secretome, PF – Secretome' protein fraction, and EXO – Exosomal fraction previously isolated from the MSCs secretome, and diluted in Neurobasal A medium. The incubation time for this experiment was 5 days and in the end, cells were fixed and an immunocytochemistry protocol was performed.

3.4.2. Immunocytochemistry of hNPCs

After 5 days in culture, the cells were fixed with paraformaldehyde (PFA) (4%) (Merck, Portugal) for 30 min at RT to conserve cellular morphology and allow protocol execution. Posteriorly, to allow binding of the antibodies to their epitopes, cells were permeabilized with a solution of PBS-Triton (0.3%) (Sigma, USA) for 5 min followed by a blockage solution (10% FCS (Biochrom, Germany) in PBS) for 1 hour at RT to ensure a greater binding specificity to the interest antigen. Cells were then incubated for 1 hour at RT with the primary antibodies (Table 2), diluted in 10% FCS in PBS. After incubation time, the cells were washed, this time with PBS with 0.5% of FCS, allowing the non-specific blockage to remain optimal. The cells were then incubated with the secondary antibodies (Table 3) diluted in 10% FCS in PBS for 1 hour at RT. Finally, cells were incubated with 4', 6-diamidino-2-phenylindole-dihydrochloride (DAPI, 1:1000, Life Technologies, USA) for 5 min at RT. Afterwards, coverslips were assembled on microscope slides using PermaFluor Aqueous Mounting Medium (Thermo Fischer Scientific, UK) and left to dry overnight at 4°C, being then visualized in an OLYMPUS BX81 fluorescence microscope. For cell quantification analysis, three coverslips and ten representative fields per coverslip were chosen and analyzed. In order to normalize the data between the different sets, the results are presented in percentage of cells. This was calculated by counting the cells positive for DCX and MAP-2 markers, and dividing this value by the total number of cells per field (DAPI-positive cells; n=3).

Table 2. Primary Antibodies

Antibody – Host	Company	Dilution
Doublecortin (DCX) – Rabbit	Abcam (UK)	1:500
Microtubule associated protein-2 (MAP-2) – Mouse	Sigma (USA)	

Table 3. Secondary Antibodies

Antibody – Antigenicity	Company	Dilution
Alexa Fluor 488 – Goat Anti-rabbit	Life Technologies (USA)	1:1000
Alexa Fluor 594 – Goat Anti-mouse		

3.4.3. DAn – derived from mESCs insult with 6-OHDA and treatment with hBM-MSCs secretome different fractions

6-OHDA (Sigma, USA) was dissolved in water containing 0.1% of ascorbic acid. Differentiated DAn-derived from mESCs were exposed to 500 μM 6-OHDA for 4 hours. After this period, the wells were washed with Neurobasal A medium. Then, the medium was replaced, and cells incubated with 5 different conditions, namely: CT^{+}- Positive control that comprises the optimal cell differentiation medium (ADFNK medium), CT^{-} –Negative control that only contains Neurobasal A medium with 1% of kanamycin, CM – MSCs secretome, PF – Secretome' protein fraction, and EXO – Exosomal fraction previously isolated from the MSCs secretome, and diluted in Neurobasal A medium. The incubation time for this experiment was 2 days and, in the end, cells viability was evaluated.

3.4.3.1. Cell viability assay by MTS method

Firstly, cells were washed once with PBS 1x (without Mg^{2+} and Ca^{2+}) and then incubated with MTS (1:5 in Neurobasal) solution for 5.5 hours at 37°C. After the incubation period, 3 replicates of 100 μL per well were retrieved to a 96-well plate and the absorbance was read at 490 nm.

3.5. *In vivo* Assay

3.5.1. Stereotaxic Surgeries

3.5.1.1. 6-OHDA Model Induction Surgeries

Nine-weeks-old Wistar-Han male rats (Charles River, Barcelona) were housed in pairs, in polycarbonate cages, and maintained in a standard controlled environment at 22-24°C RT and 55% humidity, on a 12 hours light/dark cycle, with food and water *ad libitum*. Animals were handled for 1 week before the experimental procedures, in order to reduce the stress induced by the surgical practices. All the experiments were performed under the consent from the *Ethical Subcommittee in Life Sciences and Health* (SECVS; SECVS 142/2016), and conducted in accordance with the local regulations on animal care and experimentation (European Union Directive 2010/63/EU). For surgical interventions, the animals were anesthetized with a mixture of ketamine (Imalgene, Merial, USA) and medetomidine (Dorbene, Zoetis, Spain) [75 mg/kg; 0.5 mg/kg intraperitoneally (i.p.)], placed on a stereotaxic frame (Soelting, USA), and unilaterally injected, using a 30-gauge Hamilton needle syringe (Hamilton, Switzerland), with vehicle (Sham group, n=13) or with 6-OHDA hydrochloride (Sigma, USA) (6-OHDA group, n= 52) in the medial forebrain bundle (MFB) [coordinates related to Bregma: AP= -4.4 mm, ML= -1.0 mm, DV= -7.8 mm; (Carvalho, Campos et al. 2013) (Paxinos and Watson 2007). The sham animals were injected with 2 μL of 0.2 mg/mL of ascorbic acid in 0.9% NaCl and, the 6-OHDA group of animals were injected with 2 μL of 6-OHDA hydrochloride (4 μg/μL) with 0.2 mg/mL of ascorbic acid in 0.9% of NaCl at a rate of 0.5 μL/min. After the injection, the needle was raised 0.1 mm and left in place for 2 min in order to avoid any backflow up the needle tract. Three weeks after the model induction surgery, the behavior performance of the animals was assessed.

3.5.1.2. Treatment Surgeries: Intracranial injections of hBM-MSCs Secretome, Protein Fraction, and Exosomes

Five weeks after the PD model induction, the animals were unilaterally injected in the STR and SNpc with the different fractions of the hBM-MSCs secretome, which includes the secretome itself, the protein fraction and the isolated exosomes. As previously described, for the surgical procedures: the animals were anesthetized with ketamine-medetomidine [75 mg/kg; 0.5 mg/kg (i.p.), and injected using a 30-gauge needle Hamilton syringe (Hamilton, Switzerland), with either vehicle (Neurobasal A medium; 6-OHDA control group; n=13), hBM-MSCs secretome (Secretome; n=13), hBM-MSCs protein fraction (Protein Fraction; n=13) or hBM-MSCs exosomes (Exosomes;

n=13). The animals were injected directly in the SNpc (coordinates related to Bregma: AP= - 5.3 mm, ML= -1.8 mm, DV=- 7.4 mm) and in the STR (coordinates related to Bregma: AP= -1.3 mm, ML= 4.7 mm, DV= -4.5 mm; AP= -0.4 mm, ML= 4.3 mm, DV= -4.5 mm; AP= 0.4 mm, ML= 3.1 mm, DV= -4.5 mm; AP= 1.3 mm, ML= 2.7 mm; DV= -4.5 mm) (Paxinos and Watson 2007). 6-OHDA control group was injected with 4.0 μL of Neurobasal A medium in the SNpc and 2.0 μL in each coordinate of the STR at a rate of 1 μL/min. The treated animals were injected with the same amount as the 6-OHDA-control animals but with their respective treatment (hBM-MSCs secretome, protein fraction, and exosomes). After each injection, the needle was raised 0.1 mm and left in place for 2 min in order to avoid any backflow up the needle tract. One, four, and seven weeks after these treatment surgeries, the behavior performance of the animals was assessed.

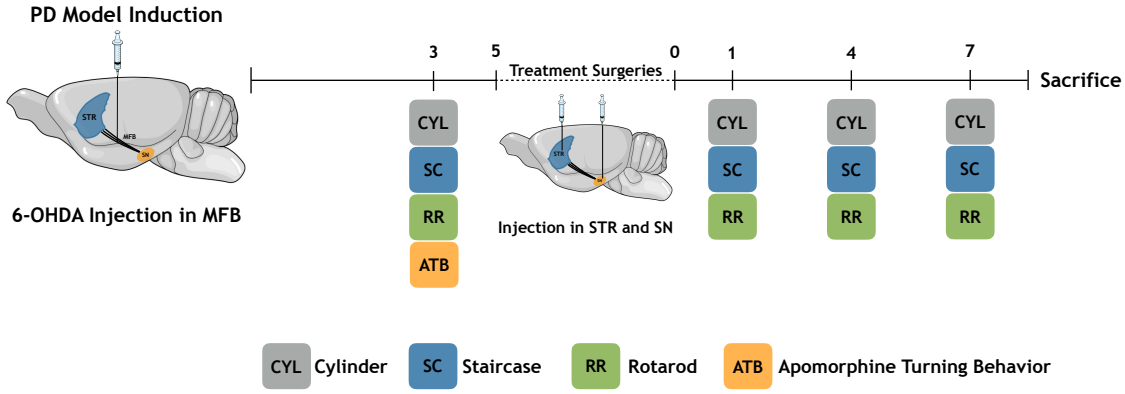

Figure 3. *In vivo* experimental design. Parkinson's disease model was induced by the unilateral injection of 6-OHDA neurotoxin in the medial forebrain bundle (MFB) of the brain of the animals. 3 weeks later a behavioral assessment was performed to validate the model through Cylinder, Staircase, Rotarod and Apomorphine turning behavioral tests. After the model validation, the animals were then submitted to a second surgery, this time comprising the injection of hBM-MSCs secretome, protein fraction, and exosomes in several coordinates of the striatum (STR) and in the substantia nigra (SN) of the animals. 1, 4 and 7 weeks after treatment surgery, animal behavior was assessed.

3.5.2. Behavioral Assessment

3.5.2.1. Rotarod Test

The animals' motor coordination and balance were assessed through the rotarod test as previously described (Monville, Torres et al. 2006). The test consists in using the Rotarod apparatus (3376-4R; TSE Systems, USA), with 7 cm diameter drums under a speeding up protocol and has the total duration of 4 days. The first 3 days were used only as training of the animals and consisted in 3 rounds of the protocol, starting at 4 rpm and reaching 40 rpm in 5 min. Animals were in rest for at least 20 mins between each round. In the fourth day, and using the same protocol, this time with 4 rounds, the apparatus recorded the animal latency to fall.

3.5.2.2. Skilled Paw Reaching Test (Staircase)

Unilateral lesions with 6-OHDA and consequent dopamine depletions in dopaminergic networks lead to movement impairments and adapted postural adjustments. To assess changes in independent forelimb reaching and grasping abilities, the animals performed a skilled paw reaching test, also known as staircase test. For this, double staircase boxes (catalog no. 80300; Campden Instruments, Lafayette, IN, http://www.campdeninstruments.com), were used (Campos, Carvalho et al. 2013). These boxes consist on a translucent compartment connected to a narrow central platform with 7 descending adjacent stairs that allow the placement of 5 sucrose pellets on each step. The rats try, for 15 min, to reach from the central platform the pellets located on the stairs, in which the success rate is correspondent to the number of pellets eaten in that period. This test requires food-deprived animals (during the test period), and all sessions were performed at the same time of the day, for 7 consecutive days. A forced choice task was performed in the last two days, in which pellets were placed in one of the sides of the stairs, forcing the rats to reach the pellets of that specific side. The forced-choice test allows the assessment of the impairments of the animals' affected side.

3.5.2.3. Cylinder Test

Forelimb use asymmetry was measured by the cylinder test. The animals were individually placed in a 20-cm diameter glass cylinder and allowed to explore freely as described in (Hernando, Requejo et al. 2019). Mirrors were placed behind the cylinder to allow a 360° view of the rat movements. Each animal was left in the cylinder for 5 min and this time was recorded and later analyzed. Independent paw touches performed with the contralateral, ipsilateral or both front limbs

were counted, as well as the assisted paw touches. The data is expressed as the percentage of (Independent Left + Simultaneous Left)/(Independent Right + Independent Left + Both Paws + Simultaneous Right + Simultaneous Left) = (Total Left Movements)/(Total Movements) x 100.

3.5.2.4. Apomorphine Turning Behavior Test (Rotameter)

Apomorphine turning behavior test, also called Rotameter is used mainly in experiments using PD animal models that display a unilateral lesion in the nigrostriatal dopaminergic system. Apomorphine, a strong dopamine receptor agonist, is a stimulator of the dopaminergic system, inducing a turning behavior in lesioned animals, providing an estimation of the lesions' degree. The animals were injected subcutaneously with a solution of 0.05 mg/kg of apomorphine hydrochloride (Sigma-Aldrich) dissolved in 1% of ascorbic acid in 0.9% NaCl and placed on metal testing containers (MED-RSS, Med Associates, Fairfax, VT, http://www.medassociates.com) for 45 min. The animal wears an adjustable harness connected to a sensor that allows the digital recording of the body rotations, allowing degenerative effect assessment.

3.5.3. Histological Analysis

12 weeks after the initial model induction surgery, the animals were anesthetized with an injection of sodium pentobarbital (Eutasil, 60mg/kg (i.p.), Ceva Saúde Animal, Portugal) and perfused with saline followed by PFA 4% diluted in PBS to fix the tissues. The animals' brains were collected and stored in PFA for 3 days and then kept in a 30% sucrose solution with 0.1% of azide until ready to further histological processing. When the brains are ready for processing - when sunk in the sucrose solution – striatal and mesencephalon coronal sections are obtained using a vibratome (VT1000S, Leica, Germany) with a thickness of 50 μm. These brain slices are then used as free-floating sections for different techniques, such as tyrosine hydroxylase immunohistochemistry.

3.5.3.1. Tyrosine Hydroxylase (TH) Immunohistochemistry

Four series of consecutive slices were obtained from the vibratome and 6 slices of each selected brain region was used for a free-floating TH-immunohistochemistry. The remaining slices were cryopreserved at -20°C in a solution of ethylene glycol and 30% sucrose. Initially, the slices were immersed in PBS with 3% of hydrogen peroxidase (H_2O_2) for 20 min in order to inhibit endogenous peroxidase activity. Then, the slices were permeabilized in 0.1% of PBS-T for 10 min followed by a blockage of 2 hours with 5% of fetal calf serum (FCS, Life Technologies) in PBS. Following this, the

slices were incubated overnight at 4°C with rabbit TH primary antibody diluted in PBS 1x with 2% of FCS (TH, 1:1000, Millipore, USA). In the following day, the slices were washed 3 times for 10 min with 0.1% PBS-T, incubated with a biotinylated secondary anti-rabbit antibody (LabVison, USA) for 30 min, and with an Avidine/Biotine complex (LabVison, USA) for another 30 min at RT. Afterwards, the slices were immersed in Tris-HCl (1x) for 10 min and the antigen visualization was performed by using 3,3'-diaminobenzidine tetrahydrochloride (DAB, Sigma, USA) (25 mg of DAB in 50 mL of Tris-HCL 0.05 M, pH 7.6 with 12.5 µL of H_2O_2) and the reaction was stopped at the desired time using Tris-HCl. In the end, the slices were mounted on superfrost slides and left to dry in the dark. After 24h, a thionin counter-coloration was performed and the slides were coverslipped using entellan (Merck KGaA, Germany).

3.5.3.2. Stereological Analysis

Four identical TH-immunostained slices covering the entire mesencephalon were chosen and stereologically analyzed. For that, a brightfield microscope (BX51, Olympus, Japan) equipped with a digital camera (PixeLINK PL-A622, CANIMPEX Enterprises Ltd., Canada) was used, and with the help of Visiopharm integrator system software (V2.12.3.0, Denmark), the borderlines of the SNpc area were drawn. The delimitation of the SNpc region was performed through identification of anatomic standard reference points and with the help of the rat brain atlas (Paxinos and Watson 2007). The analysis comprised of the total counting of TH-immunopositive cells inside the delimitated area on both hemispheres (40x magnification), and the data is presented as the percentage of remaining TH-positive cells in the lesioned side when compared to the control side. All the analysis was performed under blind conditions.

3.5.3.3. Striatal Fiber Density Measurement

Quantification of TH immunoreactivity through densitometry measures of TH-positive striatal terminals was performed on previous TH-immunostained striatal rat brain sections as described in (Febbraro, Andersen et al. 2013). To do so, striatal sections were selected (four sections per animal) and photographed (1x magnification) under bright field illumination (SZX16, Olympus, Japan) fitted with a DP-71 digital camera (Olympus, 32Japan). Photos were converted to 16-bit gray scale using the Image J software (ImageJ v1.48, National Institute of Health, USA) and analyzed for gray intensity after standardization of the program parameters. Through a rectangular grid with $1mm^2$, it was possible to determine the density values of the striatum in both

hemispheres. Measurement of the cortex density in both hemispheres allows to remove the nonspecific background. Therefore, striatal fiber densities were determined by the difference between the striatum of one hemisphere and the cortex, allowing the comparison between striatum of both hemispheres. The extent of the immunostaining on the lesioned side was expressed as a percentage of the intact side.

3.6. Statistical Analysis

Statistical evaluation was performed using IBM SPSS Statistics ver.22 (IBM Co., USA) and graph's representation using GraphPad Prism ver.6 (GraphPad Software, La Jolla, USA). To perform the evaluation of the *in vitro* assay a one-way ANOVA was used in order to compare the mean values of the five groups. Statistical analysis for behavior tests after 6-OHDA PD animal model was performed using an independent sample t-test, and repeated measures ANOVA if an evaluation along time was required. After treatments, the behavior and histological data was analyzed using two-way ANOVA to compare the mean values for the five groups. Normality was measured using the Kolmogorov-Smirnov and Shapiro-Wilk statistical tests and taking into account the respective histograms and measures of skewness and kurtosis. Equality of variances and Sphericity were measured using the Levene's and Mauchly's tests, respectively, and was assumed when $p>.05$. Multiple comparisons between groups were accomplished through the Bonferroni statistical test. Values were accepted as significant if the p-value was lower than 0.05 and all results were expressed as group mean ± SEM (standard error of the mean). Effect size was calculated using η^2 partial.

4. RESULTS

4.1. Exosomal characterization through Dynamic Light Scattering (DLS)

The size distribution of the isolated exosomes was obtained by Dynamic Light Scattering (DLS). After 6 measurements of the samples, DLS results reveal that the mean peak is 171.25 nm (Figure 4), while the z-average is 161.25 nm, providing a more reliable measure of the average size of the particles size distribution. Also, the polydispersity index (PDI) presents values of 0.6, which implies that the sample has a broad size distribution.

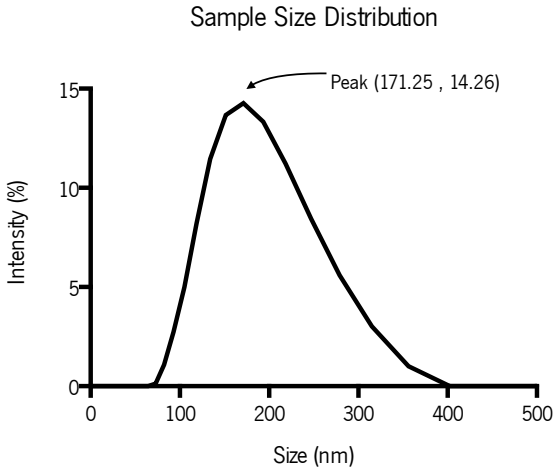

Figure 4. Characterization of the exosomal sample using Dynamic Light Scattering (DLS). Size distribution of the samples were determined by DLS in a Zetasizer Nano ZS equipment.

4.2. hBM-MSCs secretome separated fractions induced hNPCs neuronal differentiation *in vitro*

NPCs were grown as neurospheres in a serum-free medium (PPRF-h2) as previously described in (Teixeira, Carvalho et al. 2015). However, when the PPRF-h2 medium is removed, and the cells are incubated with the hBM-MSCs secretome, and with their correspondent isolated protein and exosomal fraction, the hNPCs adhered and started to differentiate. Concerning the impact of hBM-MSCs secretome different fractions on the hNPCs differentiation, results have shown distinct effects (Figure 5, Table 4). Immunocytochemistry analysis assessing neuronal differentiation to mature ($MAP\text{-}2^+$ cells) and immature (DCX^+ cells) neurons revealed that the exosomal fraction (Figure 5E, J) was able to significantly induce hNPCs differentiation at the same levels as the whole secretome (Figure 5C, H) when compared to the control group (CT^-, incubation with Neurobasal-A medium; Figure 5B, G, L, M), while the protein separated fraction was not able to induce such effect (Figure 5D, I; Table 4). Additionally, it was possible to observe

that the secretome (Figure 5C, H) and its exosomal fraction (Figure 5E, J) also induced an increased differentiation of MAP-2 and DCX positive cells when compared to the protein faction itself (Figure 5D, I, L, M).

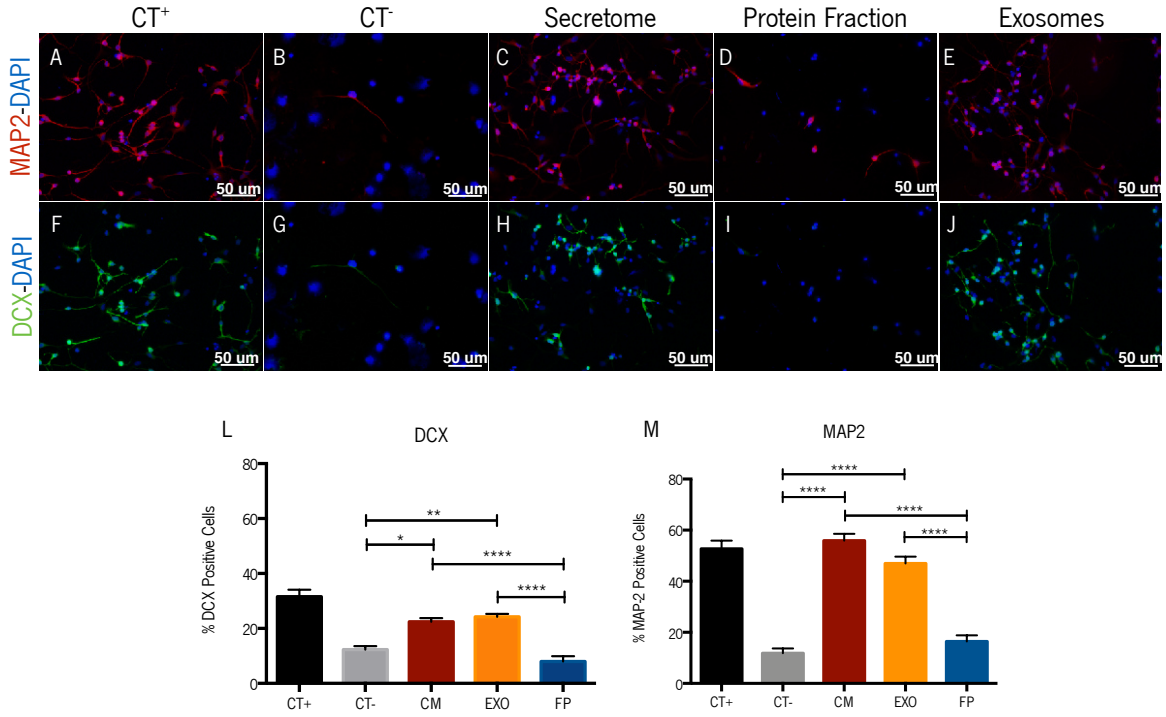

Figure 5. *In vitro* differentiation of hNPCs induced by hBM-MSCs secretome different fractions. hBM-MSCs secretome and the exosomal isolated fraction were able to significantly induce hNPCs differentiation into MAP-2^{+} cells (C, E, L) and DCX^{+} cells (H, J, M) when compared to the protein fraction (D, I) and the negative control group (B, G). Data is presented as mean ± SEM. *<.5, **, p < .01, ***, p < .001, ****<.0001.

Table 4. Statistical analysis for the hNPCs *in vitro* assay (Data presented as mean ± SEM).

Markers	CT+	CT-	CM	EXO	FP	Statistical test, significance, effect size
DCX	31.57 ± 2.561	12.32 ± 1.262	22.46 ± 1.304	24.24 ± 1.050	7.977 ± 1.897	F (4, 108) = 29.47; p <.0001; η^2=0.522
MAP-2	52.71 ± 3.210	11.82 ± 1.903	55.90 ± 2.686	47.00 ± 2.617	16.46 ± 2,350	F (4, 112) = 45.71; p<.0001; η^2=0.620

4.3. Impact of the hBM-MSCs Secretome and its Different Fractions on a 3D *in vitro* culture of Dopaminergic Neurons - derived from mouse Embryonic Stem Cells

Mouse Embryonic Stem Cells (mESCs) grow on a mouse Embryonic Fibroblasts (mEFs) feeder layer (Figure 6A) in the presence of a specific ES cell medium supplemented with LIF factor as previously described (Chumarina, Azevedo et al. 2017). Upon enzymatic digestion and plating in a low-attachment culture flask, the mESCs acquire a neurosphere-like conformation and the Embryoid Bodies (EBs) (Figure 6B) start to form through the use of a specific ADFNK differentiation medium with the supplementation of particular factors that will lead to dopaminergic cell fate. Upon individual collection and placement of the formed EBs in the collagen droplets, it is possible to verify neurite outgrowth bursting from the EBs in the collagen drops (Figure 6C).

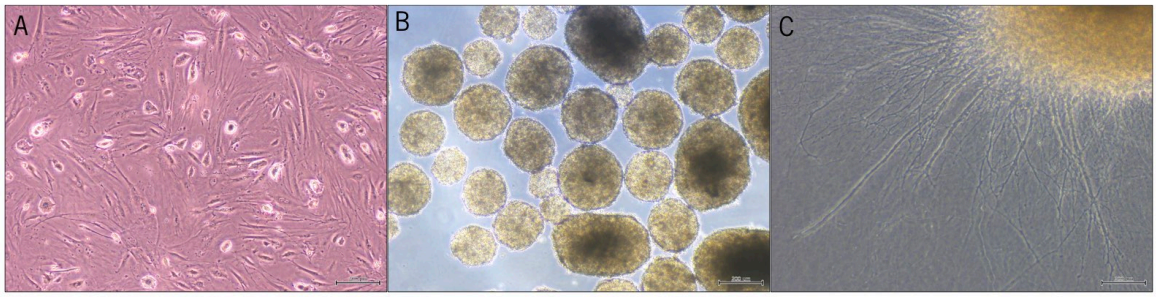

Figure 6. Expansion of dopaminergic neurons derived from mouse Embryonic Stem Cells (mESCs) *in vitro*. (A) mESCs are expanded on a mouse Embryonic Fibroblasts (mEFs) feeder layer. (B) Enzymatic digestion and plating on low-attachment flask initiates the Embryoid Bodies (EBs) formation stage. (C) Neurite outgrowth from the EBs when placed on a supportive matrix such as collagen droplets. (Scale bar: 200 μm)

4.3.1. MTS Assay

DAn-derived from mESCs were insulted with 6-OHDA toxin and treated with hBM-MSCs secretome different fractions. The impact of the hBM-MSCs secretome different fractions on DAn survival was evaluated through MTS assay. Statistical analysis show a significant effect for the factor insult, but no effect for the factor treatment nor for the interaction between these two factors (Table 5, Figure 7). Although no differences were found between treated and non-treated conditions, a positive indication was verified regarding cell viability in the cells treated with the MSCs secretome, and specially with its exosomal fraction (Figure 7).

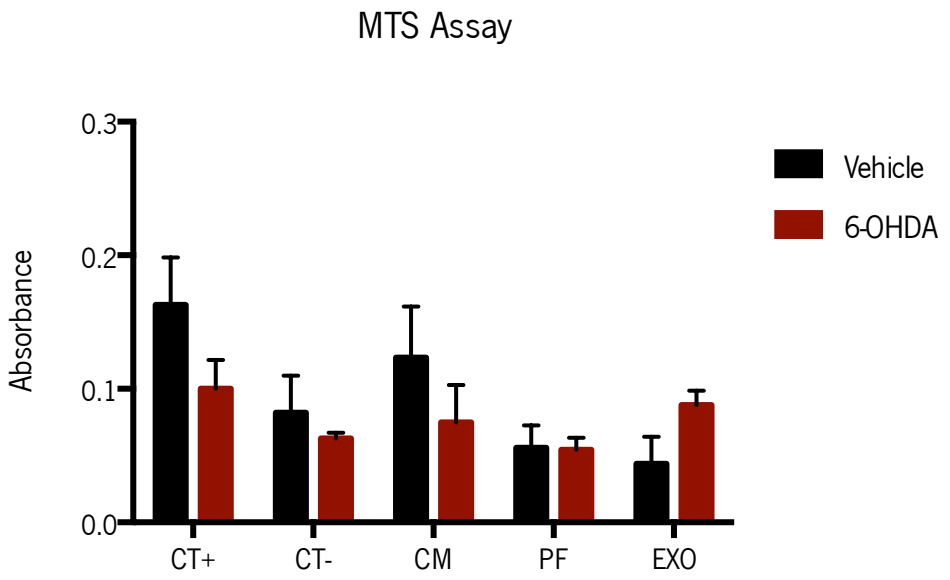

Figure 7. Impact of hBM-MSCs secretome different fractions on DAn viability through MTS assay. hBM-MSCs secretome and the exosomal isolated fraction appears to modulate cell viability levels after exposure to 6-OHDA toxin. Data is presented as mean ± SEM.

Table 5. Statistical analysis for the DAn – derived from mESCs *in vitro* assay (Data presented as mean ± SEM).

	CT+	CT-	CM	EXO	FP	Statistical test, significance, effect size
Vehicle	0.163 ± 0.066	0.082 ± 0.034	0.123 ± 0.055	0.044 ± 0.022	0.056 ± 0.025	Treatment effect: F (4, 44) = 3.075; p = 0.0256; η^2=0.194 Insult effect: F (1, 44) = 1.255; p = 0.2687; η^2=0.019 Interaction time-group: F (4, 44) = 1.432; p = 0.2394; η^2=0.091
6-OHDA	0.100 ± 0.021	0.063 ± 0.004	0.075 ± 0.031	0.088 ± 0.012	0.054 ± 0.009	

4.4. Phenotypic Characterization of the 6-OHDA rat model of PD

Three weeks after the induction surgery, behavior assessment was performed in order to identify an altered phenotype induced by the injection of 6-OHDA. Therefore, in order to address the functional integrity of the dopaminergic system, the rotameter test was performed. This test provides an estimation of the surgeries success and lesion extension, in which an increased number of net contralateral rotations correlates with a greater lesion extent. In fact, from the results it was possible to observe that there was a significant higher number of net contralateral rotations in lesioned animals when compared to the sham group (Figure 8B, Table 6). Additionally, the motor performance of the animals was also compromised by the 6-OHDA injection in the MFB. To assess skilled motor function, the staircase test was used, and results revelated that 6-OHDA-injected animals had its motor performance compromised when compared to the sham animals (Figure 8C, Table 6). Also, in a forced-choice task, 6-OHDA-injected animals had a significant impairment in the affected side (contralateral to the lesion – left side) when compared to those in the sham group (Figure 8D, Table 6). Concerning motor coordination and balance, measured by the rotarod test, results have demonstrated a significant impairment in the 6-OHDA-injected animals (Figure 8E, Table 6). Furthermore, the percentage of the impaired limb use, assessed by the cylinder test, also showed a significant decrease in the animals injected with 6-OHDA when compared to the sham group (Figure 8F, Table 6).

Table 6. Statistical Analysis of the phenotypic characterization of the 6-OHDA animal model of PD (Data presented as mean ± SEM).

Behavior Tests		Sham	6-OHDA	Statistical test, significance, effect size
Rotameter		0 ± 0	183.8 ± 18.73	t=4.876; df=63; p < .0001
RotaRod		198.3 ± 6.005	133.3 ± 1.908	t=10.31; df=6; p < .0001
Staircase	Day 1	26.48 ± 4.183	11.10 ± 1.656	Treatment effect: F (1, 63) = 26.53; p < .0001; η^2=0.215 Time effect: F (4, 252) = 62.22; p < .0001; η^2=0.118 Interaction time-group: F (4, 252) = 1.924; p = 0.1070; η^2= 0.003
	Day 2	36.48 ± 4.003	15.27 ± 1.628	
	Day 3	41.32 ± 4.794	20.66 ± 1.843	
	Day 4	46.15 ± 4.968	24.81 ± 1.888	
	Day 5	52.20 ± 5.170	28.90 ± 2.270	
Forced-choice right		55.38 ± 6.074	48.68 ± 2.822	t=1.046; df=63; p=0.2994
Forced-choice left		47.91 ± 5.278	15.05 ± 3.033	t=4.961 df=63; p < .0001
Cylinder		50.62 ± 2.087	23.07 ± 1.882	t=7.267; df=59; p < .0001

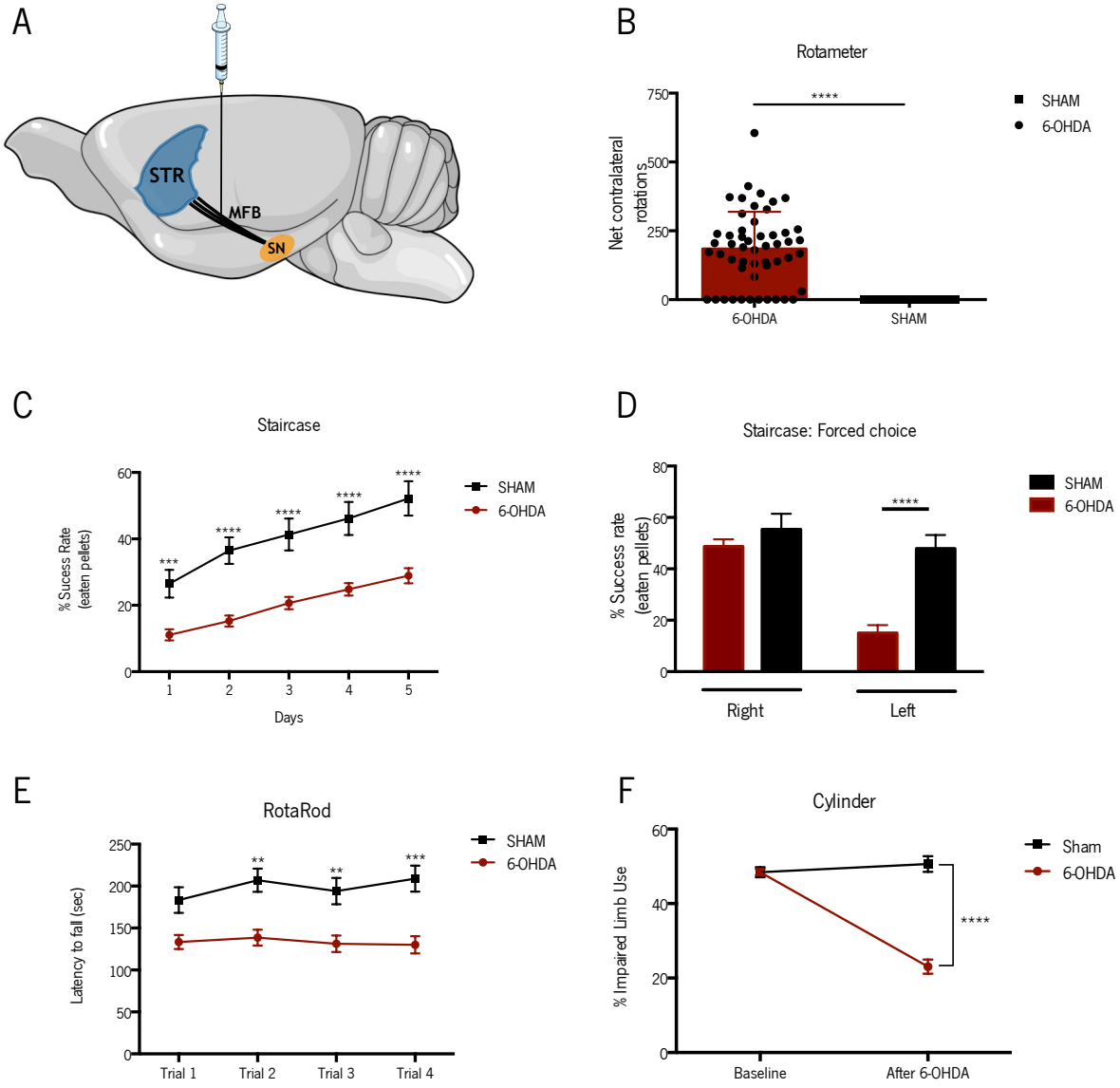

Figure 8. Behavioral characterization of 6-OHDA induced lesions. After 3 weeks, the injection of 6-OHDA in the Medial Forebrain Bundle (MFB) (A) led to a higher net contralateral rotations in the rotameter test when compared with the sham animals (B). Animals injected with 6-OHDA also demonstrated impairments in the paw-reaching test performance (C, D), in motor coordination (E), and in the use of the impaired limb (F). For rotameter test, n=13 for the sham group and n=51 for the 6-OHDA group. Data is presented as mean ± SEM. **, p < .01, ***, p < .001, ****<.0001.

4.5. Injection of the different fractions of the hBM-MSCs secretome for the treatment of the PD phenotype

To assess the effects of the hBM-MSCs secretome and its different fractions in the 6-OHDA rat model of PD, the animals motor performance was evaluated at 1, 4, and 7 weeks after the treatment surgeries through the rotarod, staircase, and cylinder tests as previously described.

4.5.1. Rotarod test

Regarding the rotarod test, ANOVA results showed a significant effect for the factor treatment, however, no effects were observed for the factor time and no interaction was achieved between both factors (Table 7). Besides the significant performance of Sham animals, further comparison showed that the animals previously lesioned and treated with all the different conditions (hBM-MSCs secretome, protein, and exosomal fraction) had a significant improvement in their motor coordination and balance when compared to the non-treated group 1 week after treatment (Neurobasal A; $p<.01$; Figure 9). Notwithstanding, 4 and 7 weeks after treatment, despite of a slight improvement when compared to the untreated group (Neurobasal-A), such differences were not observed. In addition to this, when we compared hBM-MSCs secretome derivates, no differences were observed between each other (Figure 9).

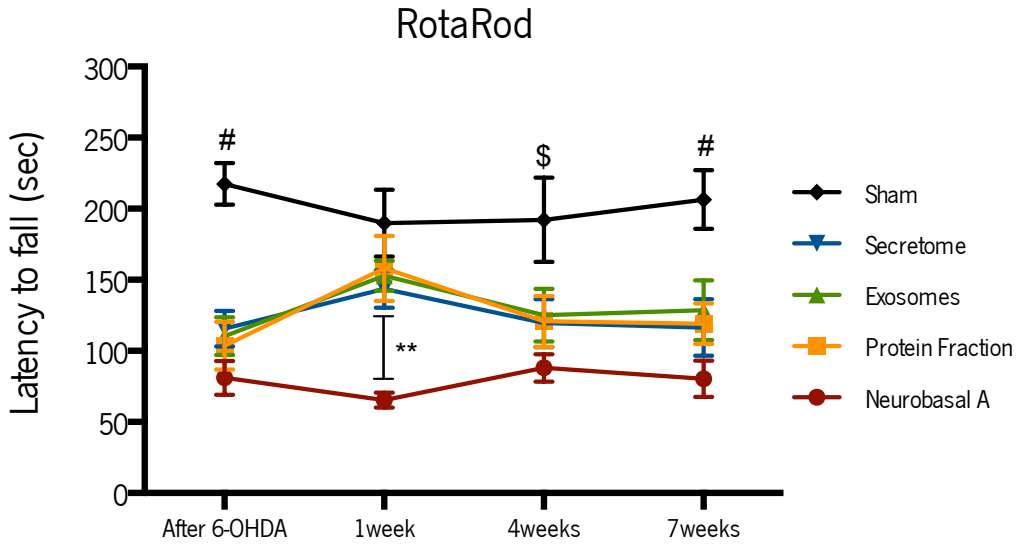

Figure 9. Motor coordination performance 1, 4, and 7 weeks after treatment with hBM-MSCs secretome, protein and exosomal fractions through a stereotaxic injection in the striatum and substantia nigra of the previously lesioned animals. Latency to fall was measured in the accelerating rotarod test, demonstrating that the animals treated with the 3 different conditions had a significant improvement in their motor coordination and balance when compared to the non-treated group at week 1. Such effect was lost at week 4 and 7. Sham: n=8, Neurobasal A: n=10, Secretome: n=13, Exosomes: n=10, Protein Fraction: n=10. Data is presented as mean ± SEM. **, $p < .01$. Sham animals statistically different from all the other groups, #p<.001. Sham group statistically different from all the other groups with the exception of the exosomes-treated animals, $.

Table 7. Statistical analysis of the rotarod test after 1, 4, and 7 weeks after treatment (Data presented as mean ± SEM).

Group	After 6-OHDA	1 Week	4 Weeks	7 Weeks	Statistical test, significance, effect size
Sham	217.4 ± 14.66	189.9 ± 23.49	192.1 ± 29.61	206.5 ± 20.51	Treatment effect: F (4. 46) = 9.823; $p < .0001$; $\eta^2 = 0.324$ Time effect: F (3. 138) = 1.655; $p = 0.1796$; $\eta^2 = 0.009$ Interaction time-group: F (12. 138) = 1.587; $p = 0.1020$; $\eta^2 = 0.035$
Neurobasal A	81.08 ± 11.87	65.44 ± 5.224	88.02 ± 9.707	80.38 ± 12.79	
Secretome	115.6 ± 12.44	143.5 ± 13.06	119.6 ± 16.84	116.5 ± 19.94	
Exosomes	110.3 ± 13.21	152.9 ± 10.52	125.1 ± 18.59	128.6 ± 21.07	
Protein Fraction	103.7 ± 16.74	158.0 ± 22.88	120.8 ± 17.86	119.2 ± 14.21	

4.5.2. Staircase test

The staircase test, as previously described, was used to assess the forelimb motor coordination of the animals, in which the success rate of eaten pellets was evaluated. Statistical analysis demonstrated a significant effect for treatment and time, but no interaction between these two factors (Table 8). Further comparison showed that lesioned animals treated with hBM-MSCs secretome had a significant improvement in their reaching abilities when compared to the untreated animals 1 week after treatment (Figure 10A). However, such effect was lost at 4 and 7 weeks after treatment. Concerning its protein and exosomal fraction *per se*, no significant effects were found when compared to the untreated group. Such result was also observed when we compared hBM-MSCs secretome, protein fraction and exosomes between each other.

Regarding the forced-choice task, in which the animals are forced to choose one of the sides of the staircase, statistical analysis revealed an effect for treatment and time, but no interaction between these two factors (Table 9 and 10, Figure 10). Considering the left side (the affected side), when we compared the animals injected with the different fractions of the hBM-MSCs secretome with the untreated group, the secretome-injected animals displayed a positive indication on the success rate of eaten pellets (Table 9, Figure 10C). Concerning the forced-choice at the right side, statistical analysis revealed an effect for time, but not for treatment, as well as no interaction (Table 10, Figure 10B).

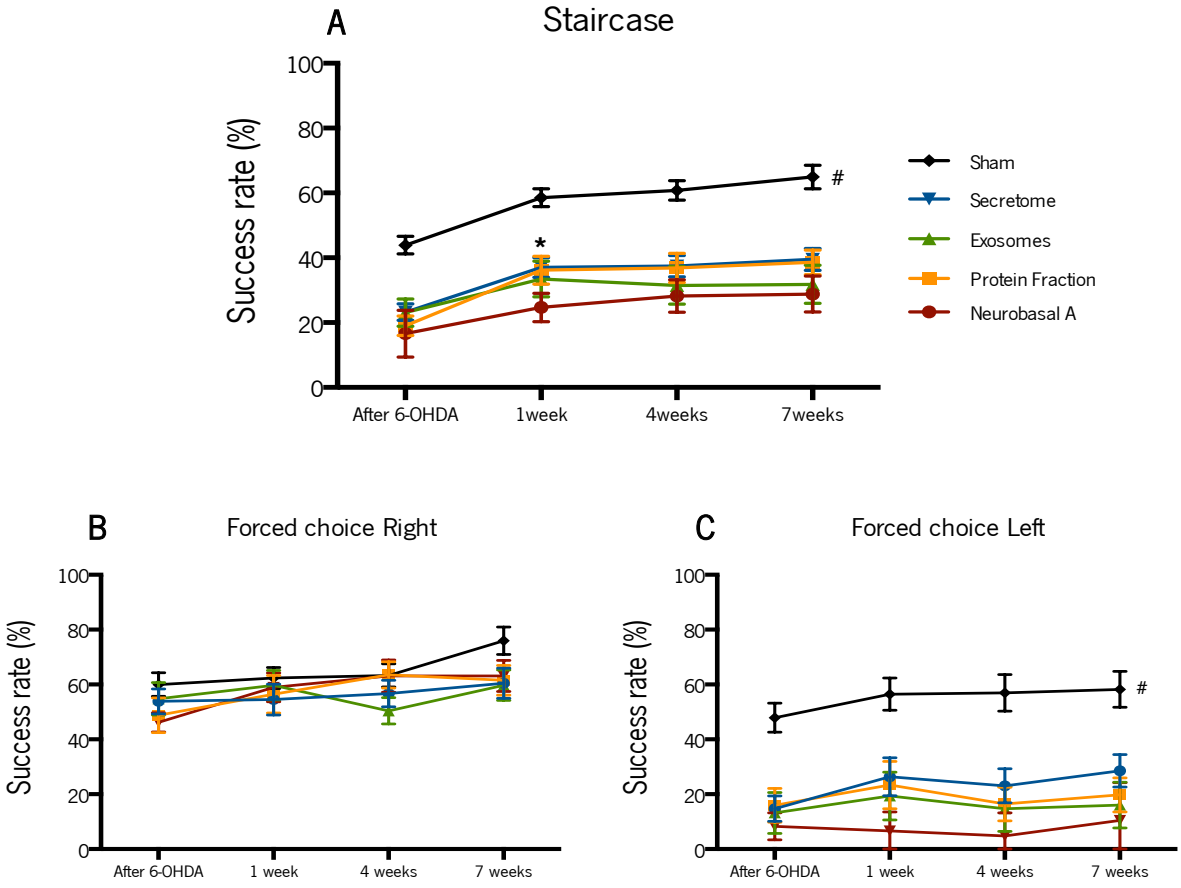

Figure 10. Impact of different secretome fractions in fine motor performance at 1, 4, and 7 weeks after treatment. (A) Paw reaching performance after 1, 4 and 7 weeks after the injection hBM-MSCs secretome, protein fraction and exosomes in the STR and SNpc. Paw reaching forced performance for (B) right and left side (C). The rats' performance is expressed as success rate of eaten pellets. Sham: n=12, Neurobasal A: n=9, Secretome: n=13, Exosomes: n=12, Protein Fraction: n=12. Data is presented as mean ± SEM. Sham animals statistically different from all the other groups, #p<.001.

Table 8. Statistical analysis of the staircase test after 1, 4, and 7 weeks after treatment (Data presented as mean ± SEM).

Group	After 6-OHDA	1 Week	4 Weeks	7 Weeks	Statistical test, significance, effect size
Sham	43.90 ± 2.716	58.51 ± 2.756	60.81 ± 2.996	64.93 ± 3.610	Treatment effect: F (4, 53) = 14.00; p < .0001; η^2= 0.378 Time effect: F (3, 159) = 54.00; p < .0001; η^2= 0.130 Interaction time-group: F (12, 159) = 1.236; p = 0.2629; η^2= 0.011
Neurobasal A	16.60 ± 2.396	24.68 ± 1.450	28.22 ± 1.672	28.82 ± 1.855	
Secretome	23.22 ± 2.548	37.01 ± 3.037	37.45 ± 3.291	39.52 ± 3.363	
Exosomes	23.10 ± 4.225	33.48 ± 5.495	31.48 ± 5.787	31.81 ± 5.886	
Protein Fraction	19.05 ± 2.979	36.19 ± 4.299	36.86 ± 4.514	38.60 ± 3.800	

Table 9. Statistical analysis of the forced choice task for the left side after 1, 4, and 7 weeks after treatment (Data presented as mean ± SEM).

Group	After 6-OHDA	1 Week	4 Weeks	7 Weeks	Statistical test, significance, effect size
Sham	47.91 ± 5.278	56.48 ± 5.869	56.92 ± 6.673	58.24 ± 6.531	Treatment effect: F (4, 55) = 9.596; p < .0001; η^2= 0.350 Time effect: F (3, 165) = 3.999; p = 0.009; η^2= 0.009 Interaction time-group: F (12, 165) = 0.6855; p = 0.763; η^2= 0.007
Neurobasal A	8.301 ± 1.639	6.667 ± 2.283	4.761 ± 2.817	10.48 ± 4.568	
Secretome	14.73 ± 4.630	26.37 ± 6.909	23.08 ± 6.235	28.57 ± 5.921	
Exosomes	13.19 ± 7.466	19.34 ± 8.681	14.73 ± 8.234	16.04 ± 8.321	
Protein Fraction	15.95 ± 6.156	23.33 ± 8.664	16.43 ± 6.103	19.76 ± 6.236	

Table 10. Statistical analysis of the forced choice task for the right side after 1, 4, and 7 weeks after treatment (Data presented as mean ± SEM).

Group	After 6-OHDA	1 Week	4 Weeks	7 Weeks	Statistical test, significance, effect size
Sham	60.00 ± 4.293	62.38 ± 3.802	63.33 ± 4.203	75.95 ± 5.004	Treatment effect: F (4, 55) = 0.7460; p = 0.5649; η^2= 0.034 Time effect: F (3, 165) = 10.45; p < .0001; η^2= 0.048 Interaction time-group: F (12, 165) = 1.796; p = 0.0525; η^2= 0.033
Neurobasal A	46.23 ± 3.506	58.96 ± 5.244	63.12 ± 5.874	63.12 ± 5.668	
Secretome	53.85 ± 4.539	54.50 ± 5.654	56.70 ± 4.807	60.44 ± 5.479	
Exosomes	54.81 ± 5.929	59.74 ± 5.386	50.39 ± 4.785	59.74 ± 5.522	
Protein Fraction	48.79 ± 6.335	56.48 ± 6.841	63.52 ± 4.778	61.54 ± 5.400	

4.5.3. Cylinder test

To assess forelimb use asymmetry, animals were placed in the cylinder test tube. Statistical analysis revealed a significant effect for time, treatment, as well as an interaction between these two factors (Table 11, Figure 11). However, although a positive indication promoted by hBM-MSCs secretome and its protein faction was observed, *post-hoc* analysis revealed no significant differences when comparing those animals with the non-treated animals (Figure 11).

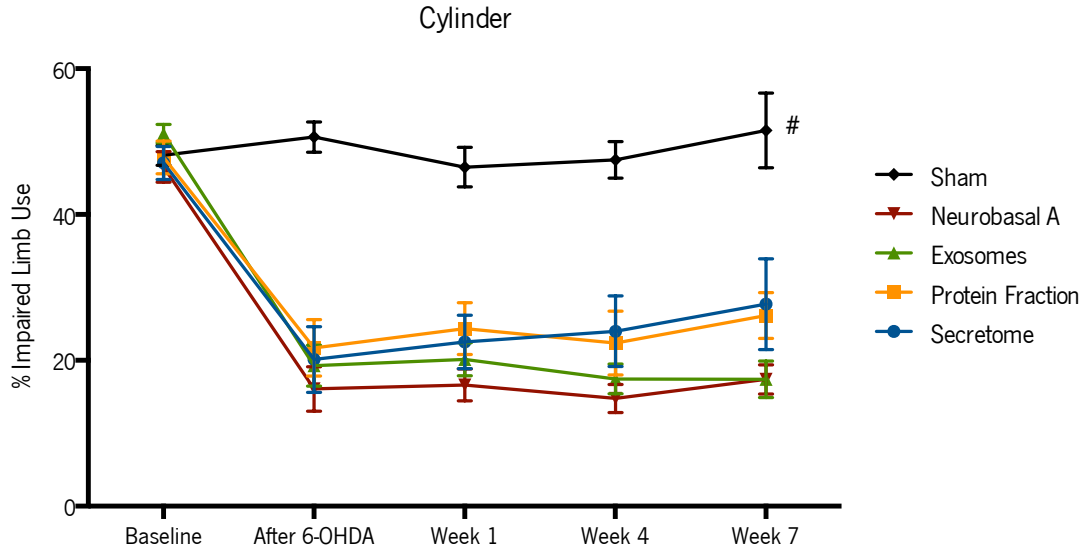

Figure 11. Impact of different secretome fractions on affected forelimb use at 1, 4 and 7 weeks after treatment. At weeks 1, 4, and 7 there was no alteration on the percentage of the affected forelimb use on the cylinder test. Sham: n=13, Neurobasal A: n=10, Secretome: n=10, Exosomes: n=10, Protein Fraction: n=10. Data is presented as mean ± SEM. Sham animals statistically different from all the other groups, # $p < .001$.

Table 11. Statistical analysis of the cylinder test after 1, 4, and 7 weeks after treatment (Data presented as mean ± SEM).

Group	Baseline	After 6-OHDA	1 Week	4 Weeks	7 Weeks	Statistical test, significance, effect size
Sham	48.13 ± 1.361	50.62 ± 2.087	46.50 ± 2.702	48.33 ± 1.327	51.54 ± 5.115	Treatment effect: $F(4, 45) = 31.91$; $p < .0001$; $\eta^2 = 0.395$ Time effect: $F(4, 180) = 76.31$; $p < .0001$; $\eta^2 = 0.247$ Interaction time-group: $F(16, 180) = 8.348$; $p < .0001$; $\eta^2 = 0.108$
Neurobasal A	47.42 ± 1.800	14.59 ± 2.663	16.63 ± 2.194	14.77 ± 1.929	17.39 ± 2.000	
Secretome	47.37 ± 2.042	20.12 ± 4.506	22.51 ± 3.660	24.00 ± 4.835	27.71 ± 6.232	
Exosomes	51.59 ± 1.299	19.62 ± 2.341	20.15 ± 2.259	17.45 ± 2.041	17.40 ± 2.522	
Protein Fraction	48.15 ± 2.021	22.29 ± 3.508	24.37 ± 3.549	22.37 ± 4.373	26.14 ± 3.134	

4.6. Assessment of the lesion extension and neuronal structure restoration

To analyze successful 6-OHDA lesions and consequent improvements with the different conditions, histological analysis for TH^+ cells and fibers were performed in the STR and in the SNpc, respectively. From the results, statistical analysis revealed that there was a significant decrease on TH-positive cells in the SNpc after the injection of 6-OHDA in the MFB (Figure 12, Table 12). Regarding the injection of the different secretome fractions, although an increase has been observed, *post hoc* analysis revealed no significant differences either between each other, either when compared to the untreated group – 6-OHDA injected with Neurobasal-A medium. The same observations were also found in the STR (Figure 13). TH-positive fibers staining was measured through a densitometry analysis and, from the results, it was possible to observe that the 6-OHDA injection led to a significant decrease of DAn fiber density (Table 13, Figure 13A-E). Concerning treatment applications, statistical analysis show that the different conditions did not lead to a significant increase of TH^+ fiber cell density in the STR when compared to the untreated group 6-OHDA (Figure 13).

Table 12. Statistical analysis of the TH-positive cells in the SNpc (Data presented as mean ± SEM).

Group	Mean ± SEM	Statistical test, significance, effect size
Sham	77.68 ± 1.664	F (4, 45) = 387.4; $p < .0001$; $\eta^2 = 0.971$
Neurobasal A	2.692 ± 0.9439	
Secretome	8.802 ± 2.811	
Exosomes	5.949 ± 1.001	
Protein Fraction	5.900 ± 0.9058	

Table 13. Statistical analysis of the TH-positive fibers in the STR (Data presented as mean ± SEM).

Group	Mean ± SEM	Statistical test, significance, effect size
Sham	80.84 ± 1.849	F (4, 58) = 78.24; $p < .0001$; $\eta^2 = 0.844$
Neurobasal A	7.792 ± 0.9054	
Secretome	17.73 ± 4.192	
Exosomes	15.35 ± 4.379	
Protein Fraction	16.00 ± 3.745	

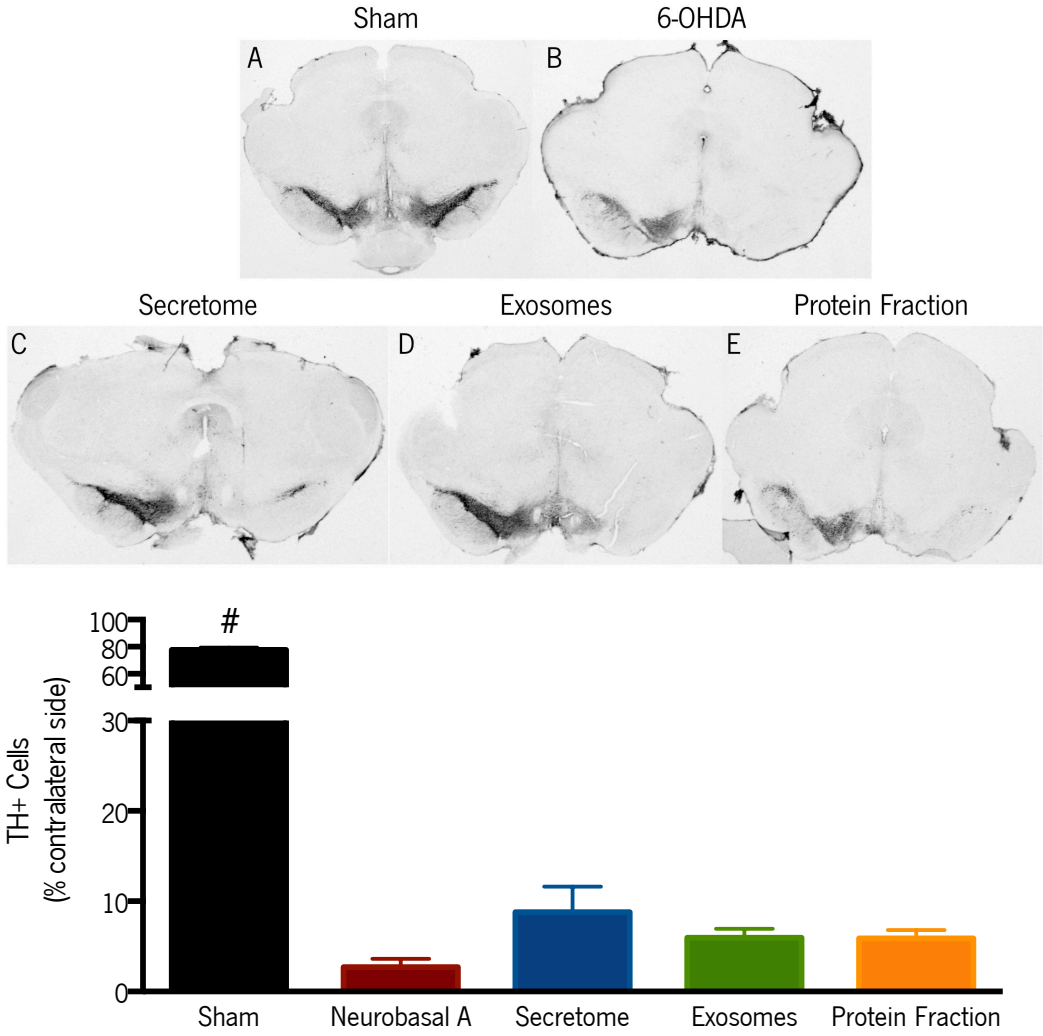

Figure 12. Representative micrographs of substantia nigra slices stained for TH. Compared to the (A) Sham group, all animals injected with 6-OHDA present a reduction of the TH positive cells (B-E). However, although an increase was observed in the treated animals, statistical analysis did not show a significant impact on TH-positive staining when compared with the untreated group 6-OHDA (B, C, D, E). Sham: n=13, 6-OHDA: n=10, Secretome: n=10, Exosomes: n=10, Protein Fraction: n=10. Data presented as mean ± SEM. #, Sham animals statistically different from all the other groups.

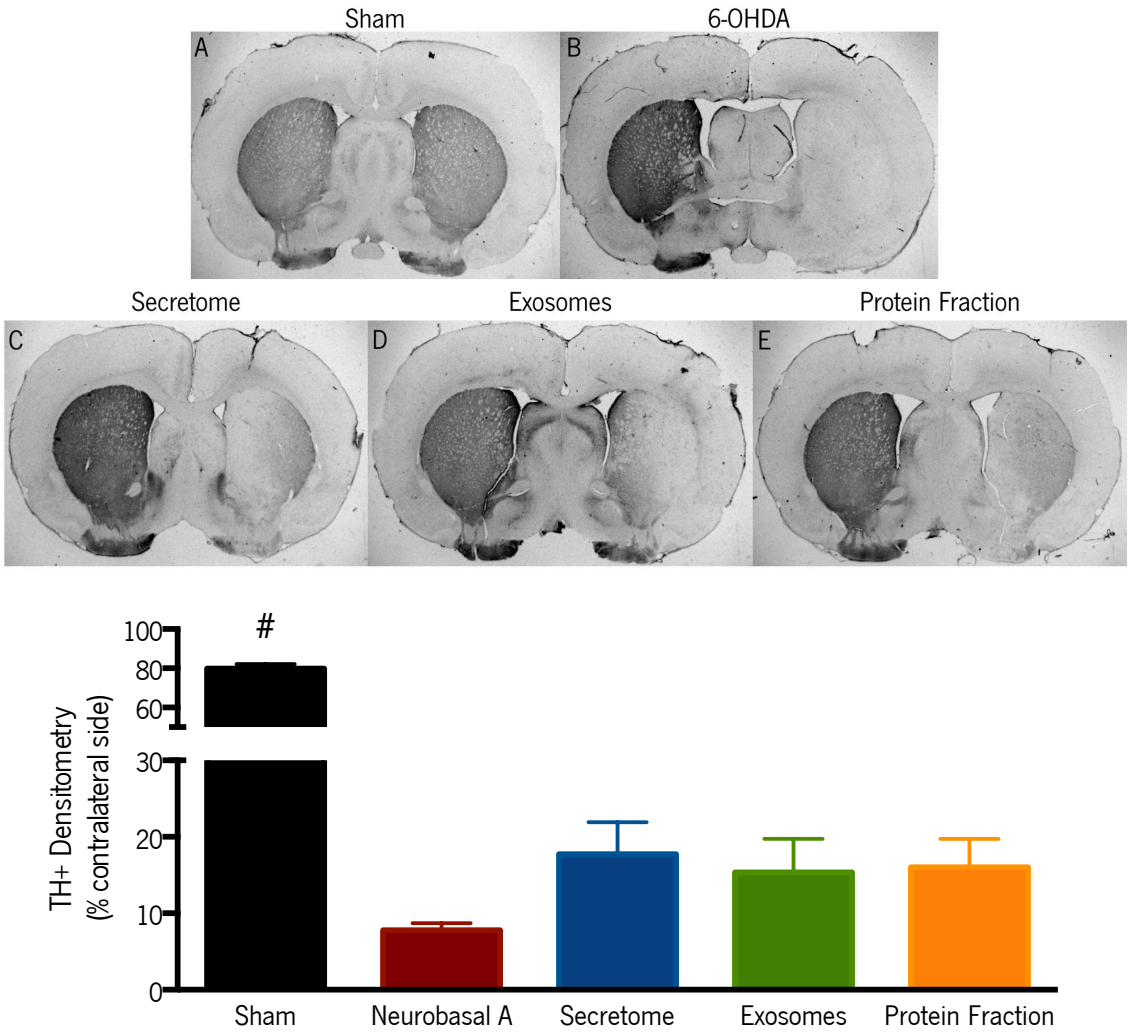

Figure 13. Representative micrographs of striatum slices stained for TH. Compared to the (A) Sham group, all animals injected with 6-OHDA present a reduction of the TH positive fibers (B-E). However, treated animals did not show a significantly higher TH-positive staining when compared with the 6-OHDA group (B, C, D, E). Sham: n=13, 6-OHDA: n=11, Secretome: n=13, Exosomes: n=13, Protein Fraction: n=13. Data presented as mean ± SEM. #, Sham animals statistically different from all the other groups.

5. DISCUSSION

Central Nervous System (CNS) disorders are one of the biggest challenges of the regenerative medicine field, as it presents a limited regeneration capacity (Williams 2014). As so, there is an increased interest in the development of new strategies and protocols aiming to treat or to slow down the progression of CNS disorders, as it is the case of PD. PD still presents no cure, since the current treatments are based on the mitigation of the core motor symptoms, rather than to stop/delay the associated neurodegenerative mechanisms or on the promotion of (DAn) regeneration (Ellis and Fell 2017). In fact, studies have been suggesting that the success of a functional recovery cannot be only associated to a single therapeutic approach, but most likely to the development and combination of multiple strategies (Chen, Shao et al. 2008, Joyce, Annett et al. 2010, Orlacchio, Bernardi et al. 2010, Viero, Forostyak et al. 2014, Williams 2014). Human Mesenchymal Stem Cells (hMSCs) have been described as a promising therapeutic tool for the treatment of several disorders, including PD (Blandini, Cova et al. 2010). Although initially it was believed that the hMSCs-mediated beneficial effects were due to their ability of transdifferentiating when transplanted, today it is known that these effects are attributed to this paracrine activity, also called secretome, which is composed of secreted soluble factors and vesicles (e.g., exosomes) (Marote, Teixeira et al. 2016). By proteomic-based analysis, apart from traditional growth factors associated with neural survival/differentiation (e.g. BDNF, GDNF, VEGF, SCF and others), our lab has also identified a pool of other neuroregulatory molecules that regulate neuroprotection, neural differentiation and axonal growth/reinnervation such as DJ-1, PEDF, Cys-C, GDN, Gal-1 (Teixeira, Panchalingam et al. 2016). Nevertheless, while with this protein soluble fraction (of hMSCs secretome) promising results were already demonstrated, the potential of its vesicular fraction remains undiscovered. Thus, on the scope of the present thesis we aimed to dissect and explore the role of the different hMSCs secretome fractions for PD regenerative medicine application, having as a major focus on the role of exosomes.

To achieve such goals, our initial experiments aimed to successfully isolate exosomes from hBM-MSCs secretome. To do so, the isolation method was based on a differential ultracentrifugation protocol, which is optimized for exosome isolation from biological fluids (Cunha, Gomes et al. 2016). When the exosomal fraction was analyzed by DLS, it was possible to verify a mean diameter peak around the supposed values for exosomes size (30-150 nm), although it has also been verified the presence of larger particles (Figure 4). Although

unexpected, such observation could be due to the presence of contaminating microvesicles or aggregates, since the DLS measurements were performed at RT, which influences the vesicles morphology (Lee, Ban et al. 2016) . Also, it is known that the EV population isolated by an ultracentrifugation technique is more heterogeneous than those isolated by using commercial kits (such as immunoprecipitation kits) (Serrano-Pertierra, Oliveira-Rodriguez et al. 2019). Indeed, this was verified by the PDI value (0.6), showing that the sample has a very broad size distribution, whereby, in the future, Nanoparticle Tracking Analysis (NTA) technique should be considered to a better sample size distribution. Additionally, and to fulfill all the criteria established by the ISEV (Lener, Gimona et al. 2015), other characterization techniques such as Western Blot (WB) and Transmission Electron Microscopy (TEM) should also be performed to ensure the purity of our vesicular/exosomal samples.

Concerning our *in vitro* experiments, which aimed to address the impact of the hBM-MSCs secretome and its different fractions on the neuronal survival and differentiation of hNPCs, the results showed that the exosomal fraction was able to induce hNPCs differentiation in different levels of neuronal maturation at the same level as the whole (hBM-MSCs) secretome when compared to a control group, while the protein separated fraction did not reach such effect, as shown in Figure 5. Picking hMSCs secretome (as a whole) effects, the observed results are in agreement with results previously described, even by our lab (Teixeira, Carvalho et al. 2015, Mendes-Pinheiro, Teixeira et al. 2018) on hNPCs differentiation and maturation. For instance, Sart and colleagues (Sart, Liu et al. 2014) reported promising effects of hMSCs secretome on hNPCs differentiation and maturation, demonstrating hMSCs secretome as a modulator of proliferation, migration and neurite extension of hNPCs, correlating such effects with the presence of important trophic factors in the secretome namely, FGF-2 and BDNF. With MSCs secretome derived from the perivascular region of the umbilical cord, Teixeira and colleagues (Teixeira, Carvalho et al. 2015) observed an increase in the survival and differentiation of hNPCs into neuronal lineages. In addition to the above-referred results, we also observed that in comparison to the protein separated fraction, hBM-MSCs secretome and its exosomal fraction were significantly better in promoting neuronal survival and differentiation of hNPCs (Figure 5). Such observations were quite surprising and puzzling since, although there is a lot of evidence showing that the paracrine factors released by MSCs are more present in small EVs (Collino, Deregibus et al. 2010, Ferguson and Nguyen 2016, Mead and Tomarev 2017), the presence of specific proteins with beneficial effects within the protein soluble fraction

implies that both may have a higher therapeutic value, and the use of the exosomal fraction alone could lead to a dilution of potentially important proteins for regeneration, thereby indicating that a kind of synergistic effect between these two fractions may exist, although such hypothesis remains to be proved. Nevertheless, it was recently demonstrated that MSCs-derived exosomes are indeed, carriers of neurotrophic factors and microRNAs with a role in hNPCs neuronal differentiation. For instance, CCL2 was found to be present in exosomes, being correlated with a stimulation of proliferation, migration, and differentiation of NPCs into neuronal and glial cells (Lee, Kang et al. 2013). In addition, miR-124 was found to be an inducer of neuronal differentiation through the suppression of Sox9 expression, leading to the loss of hNPCs multipotent capacity, and consequently, to its differentiation (Lee, Finniss et al. 2014). Although promising, the mechanisms by which exosomes interact with NPCs, and how they stimulate its neuronal differentiation, remain still poorly understood.

Under the context of disease, namely PD, we have performed an *in vitro* preliminary study by using DAn – derived from mESCs that were insulted with 6-OHDA toxin and treated with hBM-MSCs secretome different fractions. The impact on DAn survival was evaluated, and although no statistical differences were found regarding cell viability (measured by MTS), it was possible to verify a positive indication of the application of hBM-MSCs secretome and its exosomal fraction in the treated cells (Figure 7). Such indication could be explained by the fact that several studies have already demonstrated and described that hMSCs-derived exosomes have the *let*-7 microRNA family present in their internal content (Baglio, Rooijers et al. 2015). This is of great importance, since 6-OHDA is oxidized by DAn, where the primary target is mitochondria complex II, leading to an excessive production of ROS and to apoptosis induction (Mazzio, Reams et al. 2004), and the *let*-7 microRNA family present in the exosomes has been shown to have a protective role in apoptosis and autophagy (Ham, Lee et al. 2015), as well as important effects in neuronal differentiation (Meza-Sosa, Pedraza-Alva et al. 2014). In addition, it has already been demonstrated that MSCs - derived exosomes enriched in miR-133b, promote neuronal remodeling by enhancing neuritic growth, as well as functional recovery (Xin, Li et al. 2013). In fact, this is in line with what has been reported in the clinics, since it was already demonstrated that these microRNAs were found to be downregulated in PD patients (Leggio, Vivarelli et al. 2017), making them of great interest. Nevertheless, further experiments should be performed to verify the consistency of the observed results and to try to correlate

these effects with the exosomal contents trough proteomic, lipidomics, and metabolomics-based approaches, as well as microRNA levels.

Concerning the *in vivo* application of hBM-MSCs secretome and its derived fractions, like it was observed *in vitro*, distinct effects were also achieved. To dissect such assumption, we have used a well-defined rat model of PD, induced by a unilateral injection of 6-OHDA into the MFB (Carvalho, Campos et al. 2013). Such injection leads to the generation of an intracellular oxidative stress environment, inducing a massive DAn degeneration (Jackson-Lewis, Blesa et al. 2012, Gubellini and Kachidian 2015). These lesions were performed unilaterally, reducing animal loss and producing motor impairments that were easily measured after administration of dopaminergic agents, using the non-injected side as an internal control (Carvalho, Campos et al. 2013). As it has been stated, the main characteristic of this animal model is that it resembles the oxidative nature of DAn degeneration process as it occurs in human PD, leading to the appearance of the main motor symptoms of the disease. Indeed, through the rotameter test we have verified that 80% of the 6-OHDA injected animals displayed a strong turning behavior ($p<.001$) comparing with the sham group, thereby indicating that the functional integrity of the dopaminergic system was compromised. Such observations were also in accordance with animals' motor coordination performance, reaching abilities, and forelimb use, which were also affected (Figure 8). However, even being standard procedures in the characterization of PD animal models, additional assessments should also be considered, as video recording of grooming activity, and grid walk test (Chao, Pum et al. 2012), which could give a more detailed examination of the animals' behavior and the model phenotypic characterization. Still, although not conventionally performed, the analysis of the non-motor symptomatology of PD (depression, anxiety) through sucrose preference test (SPT), elevated plus maze (EPM), and forced swim test (FST) should be considered, as most of these dimensions typically precede the appearance of PD motor symptomatology (Teixeira, Gago et al. 2018). Nevertheless, this model may be too aggressive, as 3-4 days after lesion it is estimated that 70-80% of the striatal and SNpc neurons are already degenerated/lost. At the same time, and in order to really replicate a progressive phenotype over time (as it occurs in humans), the injection of 6-OHDA in the striatum should be more indicated, as it has been described that it produces a retrograde progressive degeneration of the nigrostriatal system which can last from 1-3 weeks after lesion (Alvarez-Fischer, Henze et al. 2008). Also, injections in the dorsal striatum leads to a less severe dopaminergic loss, allowing the establishment of

bilateral lesions that mimic an earlier stage of the disease (Gubellini and Kachidian 2015). Even being sustainable, to really reproduce a more realistic PD model, the injection of α-synuclein particles is recommended, which in addition of leading to DAn degeneration, also recreates one of the hallmarks of the disease, the accumulation of α-synuclein and the formation of LB (Manning-Bog, McCormack et al. 2002).

After the PD model characterization, we intended to assess the impact of hBM-MSCs secretome different fractions on the motor performance and on DAn cell survival of 6-OHDA-injected animals. Regarding the effects on motor coordination and balance, which were assessed by the rotarod test, it was possible to observe that 1 week after treatment all conditions were able to significantly improve the motor performance of the injected animals when compared to the non-treated group (Figure 9). Although better than the untreated group, 4 and 7 weeks after treatment such differences were not observed. Similar observations were also found in the staircase test (Figure 10), in which only the animals treated with the hBM-MSCs secretome had a significant improvement in their paw reaching motor coordination when compared to the non-treated group 1 week after the treatment. Curiously, and as it was observed in the rotarod, at 4 and 7 weeks after treatment these significant improvements were not achieved.

In order to assess the impact of the treatments used in this experiment in DAn integrity, histological analysis for TH-positive cells and fibers was performed and measured by cell counting and densitometry approaches, allowing an estimation of the parkinsonian lesion extent and treatment effects (Febbraro, Andersen et al. 2013). From the results, we observed an increase in TH-positive cells and fibers in the SNpc and in the STR, respectively, when compared to the untreated group (Figure 12 and 13), which in part, could be correlated with the motor performance amelioration at least 1 week after treatment. Interestingly, despite these improvements, we have also observed that the effects of hBM-MSCs secretome and its fractions declined over the time, probably through an *in situ* consumption of its contained factors and vesicles. Therefore, future studies should be performed in order to investigate the temporal effects of hBM-MSCs – derived fractions. Such results are in line with what has already been described, in which the injection of the hBM-MSCs secretome in the STR and SNpc of 6-OHDA animal models of PD was found to potentiate DAn survival and recovery, supporting the observed motor performance improvements, and the beneficial effects of the MSCs secreted factors/vesicles in PD (Teixeira, Panchalingam et al. 2016, Vizoso, Eiro et al.

2017, Mendes-Pinheiro, Teixeira et al. 2018). In fact, several protein factors have been presented as a potential explanation for the therapeutic effects of the MSCs secretome, such as BDNF, VEGF, PEDF, and GDNF, which have been described as modulators of motor and histological improvements in animal models of PD, and even in patients (Cova, Armentero et al. 2010, Venkataramana, Kumar et al. 2010, Teixeira, Panchalingam et al. 2016). Nevertheless, in addition to these molecules, hBM-MSCs secretome is also composed by exosomes, membrane-enclosed extracellular vesicles, that are involved in a complex intercellular communication system (Vilaca-Faria, Salgado et al. 2019). Concerning its application in the CNS, only few studies have already demonstrated the promising effects of MSCs secretome-derived exosomes. For instance, in Alzheimer's disease, MSCs exosomes showed to act as disease-modifying agents, leading to the degradation of β-amyloid peptides due to the presence of higher levels of neprilysin (β-amyloid degrading enzyme in the brain) on it (Katsuda, Tsuchiya et al. 2013). In PD, *in vitro* application of dental pulp-derived MSCs-exosomes were found to rescue DAn from 6-OHDA induced apoptosis, providing a potential regenerative treatment for this disorder (Jarmalaviciute, Tunaitis et al. 2015). However, as far as we know, there are no studies focusing on the application of hBM-MSCs secretome–derived exosomes in the context of PD. Nevertheless, our data showed that when applied both *in vitro* and *in vivo*, hBM-MSCs derived exosomes were able to impact neuronal survival, differentiation and viability, as well as to improve motor and histological outcomes of a 6-OHDA animal model of PD. These were interesting observations, and although a direct correlation between *in vitro* and *in vivo* data was not completely achieved, these results seem to indicate that the separation of the different secretome fractions may have distinct effects, which could open new windows of opportunities to the development of personalized strategies. Being so, although the mechanisms by which hBM-MSCs secretome and its fractions promote regenerative effects and how they can reverse the associated symptoms of PD are not fully understood, cellular and molecular analysis should be performed in order to address which signaling pathways may be modulated when hBM-MSCs secretome or its fractions are present, or even if there is a compensatory mechanism in which there is a recruitment of nearby cells that can compensate the deficits created by the parkinsonian phenotype. By doing so, this will allow the gaining of new insights about the effects of hBM-MSCs secretome fractions, and if there is an interplay between each other that could explain the data herein presented. Most likely, these facts may

open new avenues with important gains in PD therapeutics with a potential translation to the clinics.

6. CONCLUSIONS AND FUTURE PERSPECTIVES

As final remarks, the work performed in this thesis provided important insights on the interaction between the different fractions of the hBM-MSCs secretome, as well as the effects delivered by the exosomal fraction in *in vitro* and *in vivo* models of PD. In fact, although we have observed that the injection of the different secretome (as whole) fractions on a 6-OHDA animal model led to significant differences 1 week after treatment, no differences were observed between each other over the time. Actually, although several hypotheses about the secretome therapeutic potential are under investigation, further detailed studies are needed to carefully characterize and define which mechanisms may be responsible for the secretome-mediated neuroprotective and regenerative effects. For instance, by the fact that exosomes are able to cross the BBB and reach the lesioned site display a great potential in becoming a less aggressive therapy through, for example, intravenous injection. Indeed, several studies have shown that MSCs-derived exosomes act as important modulators of information between MSCs and other cells. The exchange of genetic material such as miRNA through exosomes can promote neurogenesis, reduce neuroinflammation, as well as promote functional recovery in animal models of disease, as PD. Therefore, understanding the complexity of MSCs-derived exosomes, and how its internal content interacts with the molecular and cellular PD mechanisms is of great importance. Such approach, will not only allow the exploitation of potential pathways involved in the recovery/compensation mechanisms of the disease, but also the development of multi-target-based strategies that could generate potential clinical benefits to be translated for PD patients.

7. REFERENCES

Alvarez-Fischer, D., C. Henze, C. Strenzke, J. Westrich, B. Ferger, G. U. Hoglinger, W. H. Oertel and A. Hartmann (2008). "Characterization of the striatal 6-OHDA model of Parkinson's disease in wild type and alpha-synuclein-deleted mice." Exp Neurol **210**(1): 182-193.

Anisimov, S. V. (2009). "Cell-based therapeutic approaches for Parkinson's disease: progress and perspectives." Rev Neurosci **20**(5-6): 347-381.

Arslan, F., R. C. Lai, M. B. Smeets, L. Akeroyd, A. Choo, E. N. Aguor, L. Timmers, H. V. van Rijen, P. A. Doevendans, G. Pasterkamp, S. K. Lim and D. P. de Kleijn (2013). "Mesenchymal stem cell-derived exosomes increase ATP levels, decrease oxidative stress and activate PI3K/Akt pathway to enhance myocardial viability and prevent adverse remodeling after myocardial ischemia/reperfusion injury." Stem Cell Res **10**(3): 301-312.

Asanuma, M., I. Miyazaki and N. Ogawa (2003). "Dopamine- or L-DOPA-induced neurotoxicity: the role of dopamine quinone formation and tyrosinase in a model of Parkinson's disease." Neurotox Res **5**(3): 165-176.

Assuncao-Silva, R. C., B. Mendes-Pinheiro, P. Patricio, L. A. Behie, F. G. Teixeira, L. Pinto and A. J. Salgado (2018). "Exploiting the impact of the secretome of MSCs isolated from different tissue sources on neuronal differentiation and axonal growth." Biochimie **155**: 83-91.

Baghbaderani, B. A., K. Mukhida, A. Sen, M. S. Kallos, M. Hong, I. Mendez and L. A. Behie (2010). "Bioreactor expansion of human neural precursor cells in serum-free media retains neurogenic potential." Biotechnol Bioeng **105**(4): 823-833.

Baglio, S. R., D. M. Pegtel and N. Baldini (2012). "Mesenchymal stem cell secreted vesicles provide novel opportunities in (stem) cell-free therapy." Front Physiol **3**: 359.

Baglio, S. R., K. Rooijers, D. Koppers-Lalic, F. J. Verweij, M. Perez Lanzon, N. Zini, B. Naaijkens, F. Perut, H. W. Niessen, N. Baldini and D. M. Pegtel (2015). "Human bone marrow- and adipose-mesenchymal stem cells secrete exosomes enriched in distinctive miRNA and tRNA species." Stem Cell Res Ther **6**: 127.

Beer, L., M. Mildner and H. J. Ankersmit (2017). "Cell secretome based drug substances in regenerative medicine: when regulatory affairs meet basic science." Ann Transl Med **5**(7): 170.

Bernstein, E., S. Y. Kim, M. A. Carmell, E. P. Murchison, H. Alcorn, M. Z. Li, A. A. Mills, S. J. Elledge, K. V. Anderson and G. J. Hannon (2003). "Dicer is essential for mouse development." Nat Genet **35**(3): 215-217.

Bian, S., L. Zhang, L. Duan, X. Wang, Y. Min and H. Yu (2014). "Extracellular vesicles derived from human bone marrow mesenchymal stem cells promote angiogenesis in a rat myocardial infarction model." J Mol Med (Berl) **92**(4): 387-397.

Billia, F., L. Hauck, D. Grothe, F. Konecny, V. Rao, R. H. Kim and T. W. Mak (2013). "Parkinson-susceptibility gene DJ-1/PARK7 protects the murine heart from oxidative damage in vivo." Proc Natl Acad Sci U S A **110**(15): 6085-6090.

Blandini, F., L. Cova, M. T. Armentero, E. Zennaro, G. Levandis, P. Bossolasco, C. Calzarossa, M. Mellone, B. Giuseppe, G. L. Deliliers, E. Polli, G. Nappi and V. Silani (2010). "Transplantation of undifferentiated human mesenchymal stem cells protects against 6-hydroxydopamine neurotoxicity in the rat." Cell Transplant **19**(2): 203-217.

Boyle, A. and W. Ondo (2015). "Role of apomorphine in the treatment of Parkinson's disease." CNS Drugs **29**(2): 83-89.

Braak, H., K. Del Tredici, U. Rub, R. A. de Vos, E. N. Jansen Steur and E. Braak (2003). "Staging of brain pathology related to sporadic Parkinson's disease." Neurobiol Aging **24**(2): 197-211.

Braak, H., E. Ghebremedhin, U. Rub, H. Bratzke and K. Del Tredici (2004). "Stages in the development of Parkinson's disease-related pathology." Cell Tissue Res **318**(1): 121-134.

Brodersen, P. and O. Voinnet (2009). "Revisiting the principles of microRNA target recognition and mode of action." Nat Rev Mol Cell Biol **10**(2): 141-148.

Budnik, V., C. Ruiz-Canada and F. Wendler (2016). "Extracellular vesicles round off communication in the nervous system." Nat Rev Neurosci **17**(3): 160-172.

Butcher, N. J., T. R. Kiehl, L. N. Hazrati, E. W. Chow, E. Rogaeva, A. E. Lang and A. S. Bassett (2013). "Association between early-onset Parkinson disease and 22q11.2 deletion syndrome: identification of a novel genetic form of Parkinson disease and its clinical implications." JAMA Neurol **70**(11): 1359-1366.

Campos, F. L., M. M. Carvalho, A. C. Cristovao, G. Je, G. Baltazar, A. J. Salgado, Y. S. Kim and N. Sousa (2013). "Rodent models of Parkinson's disease: beyond the motor symptomatology." Front Behav Neurosci **7**: 175.

Carvalho, M. M., F. L. Campos, B. Coimbra, J. M. Pego, C. Rodrigues, R. Lima, A. J. Rodrigues, N. Sousa and A. J. Salgado (2013). "Behavioral characterization of the 6-hydroxidopamine model of Parkinson's disease and pharmacological rescuing of non-motor deficits." Mol Neurodegener **8**: 14.

Chamberlain, G., J. Fox, B. Ashton and J. Middleton (2007). "Concise review: mesenchymal stem cells: their phenotype, differentiation capacity, immunological features, and potential for homing." Stem Cells **25**(11): 2739-2749.

Chao, O. Y., M. E. Pum, J. S. Li and J. P. Huston (2012). "The grid-walking test: assessment of sensorimotor deficits after moderate or severe dopamine depletion by 6-hydroxydopamine lesions in the dorsal striatum and medial forebrain bundle." Neuroscience **202**: 318-325.

Chen, Y., C. Gao, Q. Sun, H. Pan, P. Huang, J. Ding and S. Chen (2017). "MicroRNA-4639 Is a Regulator of DJ-1 Expression and a Potential Early Diagnostic Marker for Parkinson's Disease." Front Aging Neurosci **9**: 232.

Chen, Y., J. Z. Shao, L. X. Xiang, X. J. Dong and G. R. Zhang (2008). "Mesenchymal stem cells: a promising candidate in regenerative medicine." Int J Biochem Cell Biol **40**(5): 815-820.

Cheng, H. C., C. M. Ulane and R. E. Burke (2010). "Clinical progression in Parkinson disease and the neurobiology of axons." Ann Neurol **67**(6): 715-725.

Cho, H. J., G. Liu, S. M. Jin, L. Parisiadou, C. Xie, J. Yu, L. Sun, B. Ma, J. Ding, R. Vancraenenbroeck, E. Lobbestael, V. Baekelandt, J. M. Taymans, P. He, J. C. Troncoso, Y. Shen and H. Cai (2013). "MicroRNA-205 regulates the expression of Parkinson's disease-related leucine-rich repeat kinase 2 protein." Hum Mol Genet **22**(3): 608-620.

Chu, Y., H. Dodiya, P. Aebischer, C. W. Olanow and J. H. Kordower (2009). "Alterations in lysosomal and proteasomal markers in Parkinson's disease: relationship to alpha-synuclein inclusions." Neurobiol Dis **35**(3): 385-398.

Chumarina, M., C. Azevedo, J. Bigarreau, C. Vignon, K. S. Kim, J. Y. Li and L. Roybon (2017). "Derivation of mouse embryonic stem cell lines from tyrosine hydroxylase reporter mice crossed with a human SNCA transgenic mouse model of Parkinson's disease." Stem Cell Res **19**: 17-20.

Collino, F., M. C. Deregibus, S. Bruno, L. Sterpone, G. Aghemo, L. Viltono, C. Tetta and G. Camussi (2010). "Microvesicles derived from adult human bone marrow and tissue specific mesenchymal stem cells shuttle selected pattern of miRNAs." PLoS One **5**(7): e11803.

Cotzias, G. C., M. H. Van Woert and L. M. Schiffer (1967). "Aromatic amino acids and modification of parkinsonism." N Engl J Med **276**(7): 374-379.

Cova, L., M. T. Armentero, E. Zennaro, C. Calzarossa, P. Bossolasco, G. Busca, G. Lambertenghi Deliliers, E. Polli, G. Nappi, V. Silani and F. Blandini (2010). "Multiple neurogenic and neurorescue effects of human mesenchymal stem cell after transplantation in an experimental model of Parkinson's disease." Brain Res **1311**: 12-27.

Cunha, C., C. Gomes, A. R. Vaz and D. Brites (2016). "Exploring New Inflammatory Biomarkers and Pathways during LPS-Induced M1 Polarization." Mediators Inflamm **2016**: 6986175.

de Rivero Vaccari, J. P., F. Brand, 3rd, S. Adamczak, S. W. Lee, J. Perez-Barcena, M. Y. Wang, M. R. Bullock, W. D. Dietrich and R. W. Keane (2016). "Exosome-mediated inflammasome signaling after central nervous system injury." J Neurochem **136 Suppl 1**: 39-48.

Dexter, D. T. and P. Jenner (2013). "Parkinson disease: from pathology to molecular disease mechanisms." Free Radic Biol Med **62**: 132-144.

Dezsi, L. and L. Vecsei (2017). "Monoamine Oxidase B Inhibitors in Parkinson's Disease." CNS Neurol Disord Drug Targets **16**(4): 425-439.

Djaldetti, R., N. Lev and E. Melamed (2009). "Lesions outside the CNS in Parkinson's disease." Mov Disord **24**(6): 793-800.

Dominici, M., K. Le Blanc, I. Mueller, I. Slaper-Cortenbach, F. Marini, D. Krause, R. Deans, A. Keating, D. Prockop and E. Horwitz (2006). "Minimal criteria for defining multipotent mesenchymal stromal cells. The International Society for Cellular Therapy position statement." Cytotherapy **8**(4): 315-317.

Doxakis, E. (2010). "Post-transcriptional regulation of alpha-synuclein expression by mir-7 and mir-153." J Biol Chem **285**(17): 12726-12734.

Drago, D., C. Cossetti, N. Iraci, E. Gaude, G. Musco, A. Bachi and S. Pluchino (2013). "The stem cell secretome and its role in brain repair." Biochimie **95**(12): 2271-2285.

Ellis, J. M. and M. J. Fell (2017). "Current approaches to the treatment of Parkinson's Disease." Bioorg Med Chem Lett **27**(18): 4247-4255.

Fabbri, M., J. J. Ferreira, A. Lees, F. Stocchi, W. Poewe, E. Tolosa and O. Rascol (2018). "Opicapone for the treatment of Parkinson's disease: A review of a new licensed medicine." Mov Disord **33**(10): 1528-1539.

Febbraro, F., K. J. Andersen, V. Sanchez-Guajardo, N. Tentillier and M. Romero-Ramos (2013). "Chronic intranasal deferoxamine ameliorates motor defects and pathology in the alpha-synuclein rAAV Parkinson's model." Exp Neurol **247**: 45-58.

Ferguson, S. W. and J. Nguyen (2016). "Exosomes as therapeutics: The implications of molecular composition and exosomal heterogeneity." J Control Release **228**: 179-190.

Fraga, J. S., N. A. Silva, A. S. Lourenco, V. Goncalves, N. M. Neves, R. L. Reis, A. J. Rodrigues, B. Manadas, N. Sousa and A. J. Salgado (2013). "Unveiling the effects of the secretome of mesenchymal progenitors from the umbilical cord in different neuronal cell populations." Biochimie **95**(12): 2297-2303.

Fragkouli, A. and E. Doxakis (2014). "miR-7 and miR-153 protect neurons against MPP(+)-induced cell death via upregulation of mTOR pathway." Front Cell Neurosci **8**: 182.

Gao, F., S. M. Chiu, D. A. Motan, Z. Zhang, L. Chen, H. L. Ji, H. F. Tse, Q. L. Fu and Q. Lian (2016). "Mesenchymal stem cells and immunomodulation: current status and future prospects." Cell Death Dis **7**: e2062.

Ghebremedhin, E., K. Del Tredici, J. W. Langston and H. Braak (2009). "Diminished tyrosine hydroxylase immunoreactivity in the cardiac conduction system and myocardium in Parkinson's disease: an anatomical study." Acta Neuropathol **118**(6): 777-784.

Gomes, E. D., S. S. Mendes, R. C. Assuncao-Silva, F. G. Teixeira, A. O. Pires, S. I. Anjo, B. Manadas, H. Leite-Almeida, J. M. Gimble, N. Sousa, A. C. Lepore, N. A. Silva and A. J. Salgado (2018). "Co-Transplantation of Adipose Tissue-Derived Stromal Cells and Olfactory Ensheathing Cells for Spinal Cord Injury Repair." Stem Cells **36**(5): 696-708.

Gong, M., B. Yu, J. Wang, Y. Wang, M. Liu, C. Paul, R. W. Millard, D. S. Xiao, M. Ashraf and M. Xu (2017). "Mesenchymal stem cells release exosomes that transfer miRNAs to endothelial cells and promote angiogenesis." Oncotarget **8**(28): 45200-45212.

Groiss, S. J., L. Wojtecki, M. Sudmeyer and A. Schnitzler (2009). "Deep brain stimulation in Parkinson's disease." Ther Adv Neurol Disord **2**(6): 20-28.

Gubellini, P. and P. Kachidian (2015). "Animal models of Parkinson's disease: An updated overview." Rev Neurol (Paris). **171**(11): 750-761.

Ha, D., N. Yang and V. Nadithe (2016). "Exosomes as therapeutic drug carriers and delivery vehicles across biological membranes: current perspectives and future challenges." Acta Pharm Sin B **6**(4): 287-296.

Haining, R. L. and C. Achat-Mendes (2017). "Neuromelanin, one of the most overlooked molecules in modern medicine, is not a spectator." Neural Regen Res **12**(3): 372-375.

Halliday, G. M., Y. W. Li, P. C. Blumbergs, T. H. Joh, R. G. Cotton, P. R. Howe, W. W. Blessing and L. B. Geffen (1990). "Neuropathology of immunohistochemically identified brainstem neurons in Parkinson's disease." Ann Neurol **27**(4): 373-385.

Ham, O., S. Y. Lee, C. Y. Lee, J. H. Park, J. Lee, H. H. Seo, M. J. Cha, E. Choi, S. Kim and K. C. Hwang (2015). "let-7b suppresses apoptosis and autophagy of human mesenchymal stem cells transplanted into ischemia/reperfusion injured heart 7by targeting caspase-3." Stem Cell Res Ther **6**: 147.

Han, D., C. Wu, Q. Xiong, L. Zhou and Y. Tian (2015). "Anti-inflammatory Mechanism of Bone Marrow Mesenchymal Stem Cell Transplantation in Rat Model of Spinal Cord Injury." Cell Biochem Biophys **71**(3): 1341-1347.

Harding, C. and P. Stahl (1983). "Transferrin recycling in reticulocytes: pH and iron are important determinants of ligand binding and processing." Biochem Biophys Res Commun **113**(2): 650-658.

Hernando, S., C. Requejo, E. Herran, J. A. Ruiz-Ortega, T. Morera-Herreras, J. V. Lafuente, L. Ugedo, E. Gainza, J. L. Pedraz, M. Igartua and R. M. Hernandez (2019). "Beneficial effects of n-3

polyunsaturated fatty acids administration in a partial lesion model of Parkinson's disease: The role of glia and NRf2 regulation." Neurobiol Dis **121**: 252-262.

Hindle, J. V. (2010). "Ageing, neurodegeneration and Parkinson's disease." Age Ageing **39**(2): 156-161.

Hirsch, E., A. M. Graybiel and Y. A. Agid (1988). "Melanized dopaminergic neurons are differentially susceptible to degeneration in Parkinson's disease." Nature **334**(6180): 345-348.

Hirsch, E. C., P. Jenner and S. Przedborski (2013). "Pathogenesis of Parkinson's disease." Mov Disord **28**(1): 24-30.

Hornykiewicz, O. (1998). "Biochemical aspects of Parkinson's disease." Neurology **51**(2 Suppl 2): S2-9.

Hornykiewicz, O. (2015). "50 years of levodopa." Mov Disord **30**(7): 1008.

Im, J. H., J. H. Ha, I. S. Cho and M. C. Lee (2003). "Ropinirole as an adjunct to levodopa in the treatment of Parkinson's disease: a 16-week bromocriptine controlled study." J Neurol **250**(1): 90-96.

Jackson-Lewis, V., J. Blesa and S. Przedborski (2012). "Animal models of Parkinson's disease." Parkinsonism Relat Disord. **18**(Suppl 1): S183-185.

Jarmalaviciute, A., V. Tunaitis, U. Pivoraite, A. Venalis and A. Pivoriunas (2015). "Exosomes from dental pulp stem cells rescue human dopaminergic neurons from 6-hydroxy-dopamine-induced apoptosis." Cytotherapy **17**(7): 932-939.

Joyce, N., G. Annett, L. Wirthlin, S. Olson, G. Bauer and J. A. Nolta (2010). "Mesenchymal stem cells for the treatment of neurodegenerative disease." Regen Med **5**(6): 933-946.

Juarez Olguin, H., D. Calderon Guzman, E. Hernandez Garcia and G. Barragan Mejia (2016). "The Role of Dopamine and Its Dysfunction as a Consequence of Oxidative Stress." Oxid Med Cell Longev **2016**: 9730467.

Kabaria, S., D. C. Choi, A. D. Chaudhuri, M. M. Mouradian and E. Junn (2015). "Inhibition of miR-34b and miR-34c enhances alpha-synuclein expression in Parkinson's disease." FEBS Lett **589**(3): 319-325.

Kalani, A., A. Tyagi and N. Tyagi (2014). "Exosomes: mediators of neurodegeneration, neuroprotection and therapeutics." Mol Neurobiol **49**(1): 590-600.

Katsuda, T., R. Tsuchiya, N. Kosaka, Y. Yoshioka, K. Takagaki, K. Oki, F. Takeshita, Y. Sakai, M. Kuroda and T. Ochiya (2013). "Human adipose tissue-derived mesenchymal stem cells secrete functional neprilysin-bound exosomes." Sci Rep **3**: 1197.

Keshtkar, S., N. Azarpira and M. H. Ghahremani (2018). "Mesenchymal stem cell-derived extracellular vesicles: novel frontiers in regenerative medicine." Stem Cell Res Ther **9**(1): 63.

Kim, J., K. Inoue, J. Ishii, W. B. Vanti, S. V. Voronov, E. Murchison, G. Hannon and A. Abeliovich (2007). "A MicroRNA feedback circuit in midbrain dopamine neurons." Science **317**(5842): 1220-1224.

Kim, W., Y. Lee, N. D. McKenna, M. Yi, F. Simunovic, Y. Wang, B. Kong, R. J. Rooney, H. Seo, R. M. Stephens and K. C. Sonntag (2014). "miR-126 contributes to Parkinson's disease by dysregulating the insulin-like growth factor/phosphoinositide 3-kinase signaling." Neurobiol Aging **35**(7): 1712-1721.

Komatsu, M., S. Waguri, T. Chiba, S. Murata, J. Iwata, I. Tanida, T. Ueno, M. Koike, Y. Uchiyama, E. Kominami and K. Tanaka (2006). "Loss of autophagy in the central nervous system causes neurodegeneration in mice." Nature **441**(7095): 880-884.

Kong, M., M. Ba, C. Ren, L. Yu, S. Dong, G. Yu and H. Liang (2017). "An updated meta-analysis of amantadine for treating dyskinesia in Parkinson's disease." Oncotarget **8**(34): 57316-57326.

Krol, J., I. Loedige and W. Filipowicz (2010). "The widespread regulation of microRNA biogenesis, function and decay." Nat Rev Genet **11**(9): 597-610.

Lai, R. C., F. Arslan, M. M. Lee, N. S. Sze, A. Choo, T. S. Chen, M. Salto-Tellez, L. Timmers, C. N. Lee, R. M. El Oakley, G. Pasterkamp, D. P. de Kleijn and S. K. Lim (2010). "Exosome secreted by MSC reduces myocardial ischemia/reperfusion injury." Stem Cell Res **4**(3): 214-222.

Lee, H., J. E. Kang, J. K. Lee, J. S. Bae and H. K. Jin (2013). "Bone-marrow-derived mesenchymal stem cells promote proliferation and neuronal differentiation of Niemann-Pick type C mouse neural stem cells by upregulation and secretion of CCL2." Hum Gene Ther **24**(7): 655-669.

Lee, H. K., S. Finniss, S. Cazacu, C. Xiang and C. Brodie (2014). "Mesenchymal stem cells deliver exogenous miRNAs to neural cells and induce their differentiation and glutamate transporter expression." Stem Cells Dev **23**(23): 2851-2861.

Lee, M., J.-J. Ban, W. Im and M. Kim (2016). "Influence of storage condition on exosome recovery." Biotechnology and Bioprocess Engineering **21**(2): 299-304.

Lees, A. J. (2008). "Evidence-based efficacy comparison of tolcapone and entacapone as adjunctive therapy in Parkinson's disease." CNS Neurosci Ther **14**(1): 83-93.

Lees, A. J., J. Hardy and T. Revesz (2009). "Parkinson's disease." Lancet **373**(9680): 2055-2066.

Leggio, L., S. Vivarelli, F. L'Episcopo, C. Tirolo, S. Caniglia, N. Testa, B. Marchetti and N. Iraci (2017). "microRNAs in Parkinson's Disease: From Pathogenesis to Novel Diagnostic and Therapeutic Approaches." Int J Mol Sci **18**(12).

Lener, T., M. Gimona, L. Aigner, V. Borger, E. Buzas, G. Camussi, N. Chaput, D. Chatterjee, F. A. Court, H. A. Del Portillo, L. O'Driscoll, S. Fais, J. M. Falcon-Perez, U. Felderhoff-Mueser, L. Fraile, Y. S. Gho, A. Gorgens, R. C. Gupta, A. Hendrix, D. M. Hermann, A. F. Hill, F. Hochberg, P. A. Horn, D. de Kleijn, L. Kordelas, B. W. Kramer, E. M. Kramer-Albers, S. Laner-Plamberger, S. Laitinen, T. Leonardi, M. J. Lorenowicz, S. K. Lim, J. Lotvall, C. A. Maguire, A. Marcilla, I. Nazarenko, T. Ochiya, T. Patel, S. Pedersen, G. Pocsfalvi, S. Pluchino, P. Quesenberry, I. G. Reischl, F. J. Rivera, R. Sanzenbacher, K. Schallmoser, I. Slaper-Cortenbach, D. Strunk, T. Tonn, P. Vader, B. W. van Balkom, M. Wauben, S. E. Andaloussi, C. Thery, E. Rohde and B. Giebel (2015). "Applying extracellular vesicles based therapeutics in clinical trials - an ISEV position paper." J Extracell Vesicles **4**: 30087.

Li, Z., A. Chalazonitis, Y. Y. Huang, J. J. Mann, K. G. Margolis, Q. M. Yang, D. O. Kim, F. Cote, J. Mallet and M. D. Gershon (2011). "Essential roles of enteric neuronal serotonin in gastrointestinal motility and the development/survival of enteric dopaminergic neurons." J Neurosci **31**(24): 8998-9009.

Lotvall, J., A. F. Hill, F. Hochberg, E. I. Buzas, D. Di Vizio, C. Gardiner, Y. S. Gho, I. V. Kurochkin, S. Mathivanan, P. Quesenberry, S. Sahoo, H. Tahara, M. H. Wauben, K. W. Witwer and C. Thery (2014). "Minimal experimental requirements for definition of extracellular vesicles and their functions: a position statement from the International Society for Extracellular Vesicles." J Extracell Vesicles **3**: 26913.

Manning-Bog, A. B., A. L. McCormack, J. Li, V. N. Uversky, A. L. Fink and D. A. Di Monte (2002). "The herbicide paraquat causes up-regulation and aggregation of alpha-synuclein in mice: paraquat and alpha-synuclein." J Biol Chem **277**(3): 1641-1644.

Marote, A., F. G. Teixeira, B. Mendes-Pinheiro and A. J. Salgado (2016). "MSCs-Derived Exosomes: Cell-Secreted Nanovesicles with Regenerative Potential." Front Pharmacol **7**: 231.

Martins, L. F., R. O. Costa, J. R. Pedro, P. Aguiar, S. C. Serra, F. G. Teixeira, N. Sousa, A. J. Salgado and R. D. Almeida (2017). "Mesenchymal stem cells secretome-induced axonal outgrowth is mediated by BDNF." Sci Rep **7**(1): 4153.

Mathivanan, S., H. Ji and R. J. Simpson (2010). "Exosomes: extracellular organelles important in intercellular communication." J Proteomics **73**(10): 1907-1920.

Matsuda, W., T. Furuta, K. C. Nakamura, H. Hioki, F. Fujiyama, R. Arai and T. Kaneko (2009). "Single nigrostriatal dopaminergic neurons form widely spread and highly dense axonal arborizations in the neostriatum." J Neurosci **29**(2): 444-453.

Mazzio, E. A., R. R. Reams and K. F. Soliman (2004). "The role of oxidative stress, impaired glycolysis and mitochondrial respiratory redox failure in the cytotoxic effects of 6-hydroxydopamine in vitro." Brain Res **1004**(1-2): 29-44.

McKelvey, K. J., K. L. Powell, A. W. Ashton, J. M. Morris and S. A. McCracken (2015). "Exosomes: Mechanisms of Uptake." J Circ Biomark **4**: 7.

Mead, B. and S. Tomarev (2017). "Bone Marrow-Derived Mesenchymal Stem Cells-Derived Exosomes Promote Survival of Retinal Ganglion Cells Through miRNA-Dependent Mechanisms." Stem Cells Transl Med **6**(4): 1273-1285.

Mendes-Pinheiro, B., F. G. Teixeira, S. I. Anjo, B. Manadas, L. A. Behie and A. J. Salgado (2018). "Secretome of Undifferentiated Neural Progenitor Cells Induces Histological and Motor Improvements in a Rat Model of Parkinson's Disease." Stem Cells Transl Med **7**(11): 829-838.

Meza-Sosa, K. F., G. Pedraza-Alva and L. Perez-Martinez (2014). "microRNAs: key triggers of neuronal cell fate." Front Cell Neurosci **8**: 175.

Michel, P. P., E. C. Hirsch and S. Hunot (2016). "Understanding Dopaminergic Cell Death Pathways in Parkinson Disease." Neuron **90**(4): 675-691.

Michely, J., L. J. Volz, M. T. Barbe, F. Hoffstaedter, S. Viswanathan, L. Timmermann, S. B. Eickhoff, G. R. Fink and C. Grefkes (2015). "Dopaminergic modulation of motor network dynamics in Parkinson's disease." Brain **138**(Pt 3): 664-678.

Minones-Moyano, E., S. Porta, G. Escaramis, R. Rabionet, S. Iraola, B. Kagerbauer, Y. Espinosa-Parrilla, I. Ferrer, X. Estivill and E. Marti (2011). "MicroRNA profiling of Parkinson's disease brains identifies early downregulation of miR-34b/c which modulate mitochondrial function." Hum Mol Genet **20**(15): 3067-3078.

Monville, C., E. M. Torres and S. B. Dunnett (2006). "Comparison of incremental and accelerating protocols of the rotarod test for the assessment of motor deficits in the 6-OHDA model." J Neurosci Methods **158**(2): 219-223.

Moore, D. J., L. Zhang, J. Troncoso, M. K. Lee, N. Hattori, Y. Mizuno, T. M. Dawson and V. L. Dawson (2005). "Association of DJ-1 and parkin mediated by pathogenic DJ-1 mutations and oxidative stress." Hum Mol Genet **14**(1): 71-84.

Nakamura, Y., S. Miyaki, H. Ishitobi, S. Matsuyama, T. Nakasa, N. Kamei, T. Akimoto, Y. Higashi and M. Ochi (2015). "Mesenchymal-stem-cell-derived exosomes accelerate skeletal muscle regeneration." FEBS Lett **589**(11): 1257-1265.

Oh, S. H., H. N. Kim, H. J. Park, J. Y. Shin, D. Y. Kim and P. H. Lee (2017). "The Cleavage Effect of Mesenchymal Stem Cell and Its Derived Matrix Metalloproteinase-2 on Extracellular alpha-Synuclein Aggregates in Parkinsonian Models." Stem Cells Transl Med **6**(3): 949-961.

Orlacchio, A., G. Bernardi, A. Orlacchio and S. Martino (2010). "Stem cells: an overview of the current status of therapies for central and peripheral nervous system diseases." Curr Med Chem **17**(7): 595-608.

Pang, X., E. M. Hogan, A. Casserly, G. Gao, P. D. Gardner and A. R. Tapper (2014). "Dicer expression is essential for adult midbrain dopaminergic neuron maintenance and survival." Mol Cell Neurosci **58**: 22-28.

Pantcheva, P., S. Reyes, J. Hoover, S. Kaelber and C. V. Borlongan (2015). "Treating non-motor symptoms of Parkinson's disease with transplantation of stem cells." Expert Rev Neurother **15**(10): 1231-1240.

Paxinos, G. and C. Watson (2007). The Rat Brain, Elsevier Inc.

Phinney, D. G. (2007). "Biochemical heterogeneity of mesenchymal stem cell populations: clues to their therapeutic efficacy." Cell Cycle **6**(23): 2884-2889.

Pires, A. O., B. Mendes-Pinheiro, F. G. Teixeira, S. I. Anjo, S. Ribeiro-Samy, E. D. Gomes, S. C. Serra, N. A. Silva, B. Manadas, N. Sousa and A. J. Salgado (2016). "Unveiling the Differences of Secretome of Human Bone Marrow Mesenchymal Stem Cells, Adipose Tissue-Derived Stem Cells, and Human Umbilical Cord Perivascular Cells: A Proteomic Analysis." Stem Cells Dev **25**(14): 1073-1083.

Ponomarev, E. D., T. Veremeyko and H. L. Weiner (2013). "MicroRNAs are universal regulators of differentiation, activation, and polarization of microglia and macrophages in normal and diseased CNS." Glia **61**(1): 91-103.

Pringsheim, T., N. Jette, A. Frolkis and T. D. Steeves (2014). "The prevalence of Parkinson's disease: a systematic review and meta-analysis." Mov Disord **29**(13): 1583-1590.

Puspita, L., S. Y. Chung and J. W. Shim (2017). "Oxidative stress and cellular pathologies in Parkinson's disease." Mol Brain **10**(1): 53.

Qin, J. and Q. Xu (2014). "Functions and application of exosomes." Acta Pol Pharm **71**(4): 537-543.

Quilty, M. C., A. E. King, W. P. Gai, D. L. Pountney, A. K. West, J. C. Vickers and T. C. Dickson (2006). "Alpha-synuclein is upregulated in neurones in response to chronic oxidative stress and is associated with neuroprotection." Exp Neurol **199**(2): 249-256.

Ribeiro, C. A., J. S. Fraga, M. Graos, N. M. Neves, R. L. Reis, J. M. Gimble, N. Sousa and A. J. Salgado (2012). "The secretome of stem cells isolated from the adipose tissue and Wharton jelly acts differently on central nervous system derived cell populations." Stem Cell Res Ther **3**(3): 18.

Ribeiro, C. A., A. J. Salgado, J. S. Fraga, N. A. Silva, R. L. Reis and N. Sousa (2011). "The secretome of bone marrow mesenchymal stem cells-conditioned media varies with time and drives a distinct effect on mature neurons and glial cells (primary cultures)." J Tissue Eng Regen Med **5**(8): 668-672.

Rinne, U. K. and P. Molsa (1979). "Levodopa with benserazide or carbidopa in Parkinson disease." Neurology **29**(12): 1584-1589.

Rothfuss, O., H. Fischer, T. Hasegawa, M. Maisel, P. Leitner, F. Miesel, M. Sharma, A. Bornemann, D. Berg, T. Gasser and N. Patenge (2009). "Parkin protects mitochondrial genome integrity and supports mitochondrial DNA repair." Hum Mol Genet **18**(20): 3832-3850.

Salgado, A. J., J. S. Fraga, A. R. Mesquita, N. M. Neves, R. L. Reis and N. Sousa (2010). "Role of human umbilical cord mesenchymal progenitors conditioned media in neuronal/glial cell densities, viability, and proliferation." Stem Cells Dev **19**(7): 1067-1074.

Salgado, A. J. and J. M. Gimble (2013). "Secretome of mesenchymal stem/stromal cells in regenerative medicine." Biochimie **95**(12): 2195.

Salgado, A. J., J. C. Sousa, B. M. Costa, A. O. Pires, A. Mateus-Pinheiro, F. G. Teixeira, L. Pinto and N. Sousa (2015). "Mesenchymal stem cells secretome as a modulator of the neurogenic niche: basic insights and therapeutic opportunities." Front Cell Neurosci **9**: 249.

Santpere, G. and I. Ferrer (2009). "LRRK2 and neurodegeneration." Acta Neuropathol **117**(3): 227-246.

Saraiva, C., J. Paiva, T. Santos, L. Ferreira and L. Bernardino (2016). "MicroRNA-124 loaded nanoparticles enhance brain repair in Parkinson's disease." J Control Release **235**: 291-305.

Sart, S., Y. Liu, T. Ma and Y. Li (2014). "Microenvironment regulation of pluripotent stem cell-derived neural progenitor aggregates by human mesenchymal stem cell secretome." Tissue Eng Part A **20**(19-20): 2666-2679.

Serra, S. C., J. C. Costa, R. C. Assuncao-Silva, F. G. Teixeira, N. A. Silva, S. I. Anjo, B. Manadas, J. M. Gimble, L. A. Behie and A. J. Salgado (2018). "Influence of passage number on the impact of the secretome of adipose tissue stem cells on neural survival, neurodifferentiation and axonal growth." Biochimie **155**: 119-128.

Serrano-Pertierra, E., M. Oliveira-Rodriguez, M. Rivas, P. Oliva, J. Villafani, A. Navarro, M. C. Blanco-Lopez and E. Cernuda-Morollon (2019). "Characterization of Plasma-Derived Extracellular Vesicles Isolated by Different Methods: A Comparison Study." Bioengineering (Basel) **6**(1).

Singh, N., V. Pillay and Y. E. Choonara (2007). "Advances in the treatment of Parkinson's disease." Prog Neurobiol **81**(1): 29-44.

Sonntag, K. C. (2010). "MicroRNAs and deregulated gene expression networks in neurodegeneration." Brain Res **1338**: 48-57.

Stephen, J., E. L. Bravo, D. Colligan, A. R. Fraser, J. Petrik and J. D. Campbell (2016). "Mesenchymal stromal cells as multifunctional cellular therapeutics - a potential role for extracellular vesicles." Transfus Apher Sci **55**(1): 62-69.

Sulzer, D., C. Cassidy, G. Horga, U. J. Kang, S. Fahn, L. Casella, G. Pezzoli, J. Langley, X. P. Hu, F. A. Zucca, I. U. Isaias and L. Zecca (2018). "Neuromelanin detection by magnetic resonance imaging (MRI) and its promise as a biomarker for Parkinson's disease." NPJ Parkinsons Dis **4**: 11.

Surmeier, D. J., J. N. Guzman, J. Sanchez-Padilla and P. T. Schumacker (2011). "The role of calcium and mitochondrial oxidant stress in the loss of substantia nigra pars compacta dopaminergic neurons in Parkinson's disease." Neuroscience **198**: 221-231.

Tan, C. Y., R. C. Lai, W. Wong, Y. Y. Dan, S. K. Lim and H. K. Ho (2014). "Mesenchymal stem cell-derived exosomes promote hepatic regeneration in drug-induced liver injury models." Stem Cell Res Ther **5**(3): 76.

Tarazi, F. I., Z. T. Sahli, M. Wolny and S. A. Mousa (2014). "Emerging therapies for Parkinson's disease: from bench to bedside." Pharmacol Ther **144**(2): 123-133.

Teixeira, F. G., M. M. Carvalho, A. Neves-Carvalho, K. M. Panchalingam, L. A. Behie, L. Pinto, N. Sousa and A. J. Salgado (2015). "Secretome of mesenchymal progenitors from the umbilical cord acts as modulator of neural/glial proliferation and differentiation." Stem Cell Rev **11**(2): 288-297.

Teixeira, F. G., M. M. Carvalho, K. M. Panchalingam, A. J. Rodrigues, B. Mendes-Pinheiro, S. Anjo, B. Manadas, L. A. Behie, N. Sousa and A. J. Salgado (2017). "Impact of the Secretome of Human

Mesenchymal Stem Cells on Brain Structure and Animal Behavior in a Rat Model of Parkinson's Disease." Stem Cells Transl Med **6**(2): 634-646.

Teixeira, F. G., M. M. Carvalho, N. Sousa and A. J. Salgado (2013). "Mesenchymal stem cells secretome: a new paradigm for central nervous system regeneration?" Cell Mol Life Sci **70**(20): 3871-3882.

Teixeira, F. G., M. F. Gago, P. Marques, P. S. Moreira, R. Magalhaes, N. Sousa and A. J. Salgado (2018). "Safinamide: a new hope for Parkinson's disease?" Drug Discov Today **23**(3): 736-744.

Teixeira, F. G., K. M. Panchalingam, S. I. Anjo, B. Manadas, R. Pereira, N. Sousa, A. J. Salgado and L. A. Behie (2015). "Do hypoxia/normoxia culturing conditions change the neuroregulatory profile of Wharton Jelly mesenchymal stem cell secretome?" Stem Cell Res Ther **6**: 133.

Teixeira, F. G., K. M. Panchalingam, R. Assuncao-Silva, S. C. Serra, B. Mendes-Pinheiro, P. Patricio, S. Jung, S. I. Anjo, B. Manadas, L. Pinto, N. Sousa, L. A. Behie and A. J. Salgado (2016). "Modulation of the Mesenchymal Stem Cell Secretome Using Computer-Controlled Bioreactors: Impact on Neuronal Cell Proliferation, Survival and Differentiation." Sci Rep **6**: 27791.

Teixeira, F. G., K. M. Panchalingam, R. Assunção-Silva, S. C. Serra, B. Mendes-Pinheiro, P. Patrício, S. Jung, S. I. Anjo, B. Manadas, L. Pinto, N. Sousa, L. A. Behie and A. J. Salgado (2016). "Modulation of the Mesenchymal Stem Cell Secretome Using Computer-Controlled Bioreactors: Impact on Neuronal Cell Proliferation, Survival and Differentiation." Sci Rep.

Thome, A. D., A. S. Harms, L. A. Volpicelli-Daley and D. G. Standaert (2016). "microRNA-155 Regulates Alpha-Synuclein-Induced Inflammatory Responses in Models of Parkinson Disease." J Neurosci **36**(8): 2383-2390.

Venkataramana, N. K., S. K. Kumar, S. Balaraju, R. C. Radhakrishnan, A. Bansal, A. Dixit, D. K. Rao, M. Das, M. Jan, P. K. Gupta and S. M. Totey (2010). "Open-labeled study of unilateral autologous bone-marrow-derived mesenchymal stem cell transplantation in Parkinson's disease." Transl Res **155**(2): 62-70.

Viero, C., O. Forostyak, E. Sykova and G. Dayanithi (2014). "Getting it right before transplantation: example of a stem cell model with regenerative potential for the CNS." Front Cell Dev Biol **2**: 36.

Vilaca-Faria, H., A. J. Salgado and F. G. Teixeira (2019). "Mesenchymal Stem Cells-derived Exosomes: A New Possible Therapeutic Strategy for Parkinson's Disease?" Cells **8**(2).

Vizoso, F. J., N. Eiro, S. Cid, J. Schneider and R. Perez-Fernandez (2017). "Mesenchymal Stem Cell Secretome: Toward Cell-Free Therapeutic Strategies in Regenerative Medicine." Int J Mol Sci **18**(9).

Wahid, F., A. Shehzad, T. Khan and Y. Y. Kim (2010). "MicroRNAs: synthesis, mechanism, function, and recent clinical trials." Biochim Biophys Acta **1803**(11): 1231-1243.

Wang, G., J. M. van der Walt, G. Mayhew, Y. J. Li, S. Zuchner, W. K. Scott, E. R. Martin and J. M. Vance (2008). "Variation in the miRNA-433 binding site of FGF20 confers risk for Parkinson disease by overexpression of alpha-synuclein." Am J Hum Genet **82**(2): 283-289.

Warner, T. T. and A. H. Schapira (2003). "Genetic and environmental factors in the cause of Parkinson's disease." Ann Neurol **53 Suppl 3**: S16-23; discussion S23-15.

Williams, A. (2014). "Central nervous system regeneration–where are we?" QJM **107**(5): 335-339.

Xin, H., M. Katakowski, F. Wang, J. Y. Qian, X. S. Liu, M. M. Ali, B. Buller, Z. G. Zhang and M. Chopp (2017). "MicroRNA cluster miR-17-92 Cluster in Exosomes Enhance Neuroplasticity and Functional Recovery After Stroke in Rats." Stroke **48**(3): 747-753.

Xin, H., Y. Li, B. Buller, M. Katakowski, Y. Zhang, X. Wang, X. Shang, Z. G. Zhang and M. Chopp (2012). "Exosome-mediated transfer of miR-133b from multipotent mesenchymal stromal cells to neural cells contributes to neurite outgrowth." Stem Cells **30**(7): 1556-1564.

Xin, H., Y. Li, Y. Cui, J. J. Yang, Z. G. Zhang and M. Chopp (2013). "Systemic administration of exosomes released from mesenchymal stromal cells promote functional recovery and neurovascular plasticity after stroke in rats." J Cereb Blood Flow Metab **33**(11): 1711-1715.

Xin, H., Y. Li, Z. Liu, X. Wang, X. Shang, Y. Cui, Z. G. Zhang and M. Chopp (2013). "MiR-133b promotes neural plasticity and functional recovery after treatment of stroke with multipotent mesenchymal stromal cells in rats via transfer of exosome-enriched extracellular particles." Stem Cells **31**(12): 2737-2746.

Xiong, R., Z. Wang, Z. Zhao, H. Li, W. Chen, B. Zhang, L. Wang, L. Wu, W. Li, J. Ding and S. Chen (2014). "MicroRNA-494 reduces DJ-1 expression and exacerbates neurodegeneration." Neurobiol Aging **35**(3): 705-714.

Zhang, B., Y. Yin, R. C. Lai, S. S. Tan, A. B. Choo and S. K. Lim (2014). "Mesenchymal stem cells secrete immunologically active exosomes." Stem Cells Dev **23**(11): 1233-1244.

Zhang, W., K. Phillips, A. R. Wielgus, J. Liu, A. Albertini, F. A. Zucca, R. Faust, S. Y. Qian, D. S. Miller, C. F. Chignell, B. Wilson, V. Jackson-Lewis, S. Przedborski, D. Joset, J. Loike, J. S. Hong, D. Sulzer and L. Zecca (2011). "Neuromelanin activates microglia and induces degeneration of dopaminergic neurons: implications for progression of Parkinson's disease." Neurotox Res **19**(1): 63-72.

Zhang, Y., M. Chopp, Y. Meng, M. Katakowski, H. Xin, A. Mahmood and Y. Xiong (2015). "Effect of exosomes derived from multipluripotent mesenchymal stromal cells on functional recovery and neurovascular plasticity in rats after traumatic brain injury." J Neurosurg **122**(4): 856-867.

Zhang, Z. and Y. Cheng (2014). "miR-16-1 promotes the aberrant alpha-synuclein accumulation in parkinson disease via targeting heat shock protein 70." ScientificWorldJournal **2014**: 938348.

Zhou, C. Q., S. S. Li, Z. M. Chen, F. Q. Li, P. Lei and G. G. Peng (2013). "Rotigotine transdermal patch in Parkinson's disease: a systematic review and meta-analysis." PLoS One **8**(7): e69738.

Zhou, Y., M. Lu, R. H. Du, C. Qiao, C. Y. Jiang, K. Z. Zhang, J. H. Ding and G. Hu (2016). "MicroRNA-7 targets Nod-like receptor protein 3 inflammasome to modulate neuroinflammation in the pathogenesis of Parkinson's disease." Mol Neurodegener **11**: 28.

Zhou, Y., H. Xu, W. Xu, B. Wang, H. Wu, Y. Tao, B. Zhang, M. Wang, F. Mao, Y. Yan, S. Gao, H. Gu, W. Zhu and H. Qian (2013). "Exosomes released by human umbilical cord mesenchymal stem cells protect against cisplatin-induced renal oxidative stress and apoptosis in vivo and in vitro." Stem Cell Res Ther **4**(2): 34.